PRESSURE TRANSIENT ANALYSIS OF HYDRAULICALLY FRACTURED WELLS IN MULTILAYERED RESERVOIRS

A THESIS
Presented to the Graduate Faculty
Of African University of Science and Technology

In Partial Fulfillment of the Requirements
For the Degree of

Master of Science in Petroleum Engineering

By
Shaibu Mohammed

Abuja, Nigeria

December, 2011.

PRESSURE TRANSIENT ANALYSIS OF HYDRAULICALLY FRACTURED WELLS IN MULTILAYERED RESERVOIRS

by

Shaibu Mohammed

RECOMMENDED:

Prof. Djebbar Tiab – Committee Chair

Dr. Alpheus Igbokoyi– Committee Member

Prof. Samuel Osisanya – Committee Member

APPROVED:

Chair, Department of Petroleum Engineering

Academic Provost

Date

ABSTRACT

New equations for bilinear, formation linear and pseudo-radial flow regimes in an infinite commingled fractured multilayered reservoir have been developed. The equations have been extended to Tiab's Direct Synthesis Technique that makes it easy to estimate the individual layer properties without type curve matching.

Regardless of the flow regime, the rate normalized pressure derivative with respect to the appropriate time function has been found analytically to be constant, which depicts a horizontal line on the derivative curve. This precludes the need to calculate the slope as is conventionally done and aids in easy model diagnosis or system identification and estimation of layered parameters. Dimensionless pressure and pressure derivative functions which were derived by Bennet et al[1] for an infinite commingled fractured multilayered reservoir have been extended to Tiab's Direct Synthesis Technique to evaluate the average fracture and layer properties without type curve matching. These equations make it possible to predict the pressure response of a fractured multilayered commingle reservoir.

A procedure for estimating the individual layered properties without type curve matching is included. This procedure is applicable to the interpretation of pressure and pressure derivative analysis, rate and rate derivative analysis, rate normalized pressure and derivative analysis and deconvolution both in real space and Laplace space.

ACKNOWLEDGEMENT

All thanks and praises belong to ALLAH who has been so gracious and, granted me wisdom to reach this far in the academic field.

I would wish to express my profound gratitude to my supervisor, Prof. Djebbar Tiab for his encouragement, efficient monitoring and advice despite all odds throughout the period of this work.

To my faculty, Dr. S. Osisanya, Dr. Debamista Mira, Dr. Ogbe, Prof. G. Chukwu, Mr. B. Fadase, Mrs. Franc Osseo Asare, Dr. A. Igbokoyi, Prof. D. Akpah, Prof. Illedare, and Mr. Franc Egbon; thank you all for imparting knowledge and for believing in me and bringing out the best in me throughout my stay in AUST.

To Azeb and Titus, I say thank you so much for your support. To the Petroleum Engineering class, thank you.

Finally, to my beloved parents, Sakinatu Shaibu and Sani Mohammed, thank you for bringing me up in Islamic doctrine as well as supporting my education.

DEDICATION

To my parents, Sakinatu Shaibu and Sani Mohammed.

TABLE OF CONTENTS

LIST OF FIGURES

LIST OF TABLES

CHAPTER 1 INTRODUCTION

1.1 Problem Definition

Interpretation models cannot be used effectively in multilayered reservoir until a model has been identified for each layer. In multilayered reservoirs, the pressure and pressure derivative do not display the characteristics shapes and slopes of the individual layer model response. This is because, the wellbore pressure is sensitive to the total system and hence pressure data alone cannot be used directly for layer model identification and subsequent estimation of layer properties. Consequently, using parameters derived from pressure data alone to forecast production may lead to erroneous estimation of production. Additionally, wellbore storage effect distorts pressure data which masks early flow regimes and inhibits the estimation of the layered properties. Moreover, in multilayered reservoir, each layer contributes to production at varying rates at different times. In this regard, using the total flow rate at the surface to estimate the individual layer properties is erroneous. It is necessary therefore to measure the flow rate of each layer downhole and use the layer flow rate with the pressure data for layer parameters estimation. The pressure data and flow rate of the individual layers can be converted into an equivalent pressure response that would have been obtained if the well were producing at a constant flow rate.

Correspondents have shown that in many cases, zones in layered reservoir are stimulated individually, and the layers are then commingled[3]. In addition, some layers may be fractured while others may not be at all. In this regard, different layers may have varying flow regimes especially, at early times. Therefore, assuming a single model for all the layers is certainly erroneous and may lead to wrong estimation of the layered properties. Also, due to water and gas

coning, the topmost and bottom layers may be partially fractured while the intermediate layers may be fully fractured. The equations governing flow regimes in fully fractured layer vary from those in partially fractured layers. Hence, individual layer model is essential for characterization of layered reservoir.

Equations ought to be developed to address the above problems and to estimate the parameters of fractured and unfractured layers in commingled multilayered reservoir.

1.2 Objectives

The objectives of this thesis are in two folds:

1. To derive equations to govern the flow regimes and estimate the layer properties in an infinite fractured commingled reservoirs
2. To extend the Tiab's Direct Synthesis (TDS) technique to fractured commingled multilayered reservoirs to estimate the properties of the individual layers.

1.3 Scope of the Work

Chapter 1 introduces the concept contained in this research. It explains the problems being considered and methods to solve them. The objective of this research is also captured in this chapter. Chapter 2 gives a review of the relevant literature and further explains the testing procedures in multilayered reservoir. The types of multilayered reservoir are also discussed in this chapter. Chapter 3 considers the mathematical formulation of the analytical equations governing the different flow regimes and the extension of these equations to Tiab's Direct Synthesis Technique. Chapter 4 considers the applications of the mathematical models derived in chapter 3, and subsequent estimation of the individual layer properties. Chapter 5 discusses the results and derivations. Chapter 6 presents the conclusion and recommendations for further research.

CHAPTER 2 LITERATURE REVIEW

2.1 Introduction

Knowledge of individual layer properties in multilayered reservoirs is essential for making developmental strategies. It plays a significant role in secondary recovery in that it predicts quite accurately the production forecast and, layers that have not contributed significantly to production to serve as targets for subsequent recovery. The challenge in the characterization of layered reservoir lies in a large number of unknown layer parameters especially if some or all the layers are fractured. Hence, a complete characterization of layered reservoir includes an adequate model for each layer. Different flow regimes in each layer complicate the adequate estimation of the layer properties. Often, measurements of both down-hole rates versus depth in addition to wellbore pressure are required in order to ascertain the response of each layer. Down-hole flow rate measurements are necessary to determine producing zones to estimate layer parameters. The pressure data and flow rate of the individual layers can be converted into an equivalent pressure response that would have been obtained if the well were producing at a constant flow rate.

2.2 Previous Work

Bennet et al[1] showed that for a fractured well in a commingled multilayered reservoir, the measured flow rate at the wellbore at early time (before pseudo-radial flow) is a function of the fracture properties rather than those of the reservoir but then the measured flow rate becomes a function of the reservoir flow capacity only during the pseudo-radial flow regime. The latter argument was suggested by Lefkovitz et al[7]. Bennet et al[2] studied infinite-acting multilayered reservoir with finite conducting fracture. They used the concept of dimensionless reservoir conductivity to show that commingled reservoir solutions are identical to single-layer solutions

throughout the infinite period. They determined that multilayer solutions match the single-layer solution when the dimensionless wellbore pressure is plotted as a function of t_D $C_{RD}{}^2$ for given values of dimensionless fracture conductivities during the infinite-acting period. Camacho et al[3] studied the transient pressure response of wells producing from non-communicating layered reservoir with unequal fracture length. Their work was an extension of that of Bennet et al[1]. They determined that for fractures in communication only at the wellbore, the solution for a fractured well producing from a commingled system is identical to the corresponding single layer if equivalent fracture half-length and equivalent fracture conductivity are used in the plotting functions. Lefkovitz et al[7] studied the behavior of bounded reservoir composed of stratified layers. They suggested that the fractional layer flow rate is a function of the flow capacities of the layers. Their work also showed that the time necessary to reach pseudo-steady state is much longer for a two-layer reservoir than for a single layer reservoir. Their analysis of the buildup curve showed that it is possible to determine the flow capacities of the layers, wellbore co-efficient and static reservoir pressure. Ehlig-Economides and Joseph[15] derived an equation for a layered reservoir. They used the analytic solution to determine layer properties using pressure and down-hole rate data. Their solution included wellbore storage and, cross-flow may or may not occur in adjacent layers. Their solution however, did not include induced fractures. Ehlig Economides[18] summarized multilayer reservoir testing techniques that field tests have shown to be successful. She showed that layered reservoir test relies on a combination of measurements, including production log surveys, pressure and flow rate transient acquired with the sensors maintained in a stationary position. She explained the principle behind Selective Inflow Performance Techniques and emphasized that it is necessary to achieve a stabilized flow in the well for several surface injection or production rates. She suggested that it is useful to run a

conventional pressure buildup test at the end of the Layered Reservoir Test (LRT). She further explained the two techniques that have been used for the multilayer test techniques. The first technique evaluates each zone sequentially starting with the lowest zone while the second technique uses one four-zone single well model and showed that all four of the flow periods are matched simultaneously and the measured pressure transients are used as the wellbore boundary conditions. She concluded that the LRT interpretation provides a means for the determination of individual layer properties. Kuchuk et al[25] suggested that for a layered reservoir, the parameters of the individual layers can be estimated by a sequential drawdown test in which wellbore pressure and layer flow rates are recorded simultaneously. Their work was limited to a two-layer model in a commingle reservoir. Kuchuk et al[39] applied convolution and used nonlinear regression techniques to fit the measured down-hole flow rate or pressure data with a layered reservoir model. They presented two techniques for the estimation of layer parameters. The first is the sequential analysis which involves analysis of each flow test starting from the bottom layer. The second involves the simultaneous nonlinear estimation which fits all measured down-hole flow rates to a numerical reservoir model behavior. Otuomagie and Menzie[26] extended Hartsock's pressure equation to obtain an expression for pressure buildup in an infinite two-layered commingled reservoir that can be used to determine the reservoir parameters. The equations they developed can be used to determine the initial pressure of one zone if that of the other zone is known or if the difference between the initial pressures of the two zones is known. They investigated the effects of wellbore storage. They emphasized that the force of gravity is essential if one wants to obtain equations to compute reservoir parameters of an infinite-two layered reservoir. They suggested that the pressure buildup curves obtained for an infinite two-layered reservoir without the effects of wellbore storage are similar to those of an ideal single-

layer reservoir. They showed that if the properties of the fluid are equal in both layers, the ratio becomes insignificant, and thus, an infinite two-layered reservoir behaves like a single-layer reservoir. They then concluded that the permeability and thickness ratio for an infinite two-layered reservoir do not affect the slope of the buildup curves, but the average flow capacity does. Bourdet[27] investigated the pressure behavior of layered reservoir with cross-flow. He presented an analytical solution that describes the pressure response of a well intercepting a layered reservoir with cross-flow. He showed that double porosity behavior is a limiting form of the new solution. He further showed that the double permeability model yields all intermediate behavior between the homogenous type response and that of double porosity. He suggested that the new model demonstrates that the applicability of double porosity model for layered reservoir is very restrictive. He concluded that interpretation of pressure response of a layered reservoir is often not unique and that several configurations can produce similar responses that match the data equally well. Gao[29] presented an interpretation theory for drawdown and buildup tests, which is given to individual layer of a multilayer reservoir with cross-flow. He showed that both drawdown and buildup curves have two straight lines with transition period between them. He suggested that the first straight line period determines the flow capacity and skin factor of the test layer and the second straight line determines the total flow capacity of the reservoir. He further showed that the vertical permeability of the shale between the layers can be obtained by the three analytical methods; the cross-point of the two straight lines of drawdown and buildup curves, the steady wellbore pressure difference between the test layers and the closed layers and the wellbore pressure in the early transition period respectively. Gao[35] showed that the individual layer properties of a multilayer reservoir with or without crossflow can be determined by one drawdown test if all the layers are tested together and the common wellbore pressure and the

flow rate for each layer are measured and analyzed simultaneously. He concluded that there are two causes of crossflow. One is caused by different boundary pressures for different layers while the other is caused by different diffusivities for different layers. Osman[32] developed an analytical solution to the pressure behavior of a well in a multilayered infinite acting reservoir intercepted by a finite conductivity vertical fracture. He showed that the dimensionless pressure function and its derivative are strong functions of fracture conductivity during the early time. He suggested that layer fractional production rate is a good measure of reservoir and fracture characteristics. He generated type curves for wellbore pressure and its derivative. He concluded that the effect of transmissibility and storativity on pressure behavior is found to be insignificant for all cases, but found that the effect is significant with pressure derivative. He showed that both functions are affected by fracture conductivity during early time and suggested that such effect diminishes with time. Shah et al[37] proposed a multistep testing procedure that involves down hole measurements of the pressure and fluid flow rate. They presented a multistep drawdown test involving down hole pressure and flow rate measurements for determining the layer skin and permeabilities in the layer reservoir. They suggested an approach for simultaneous analysis of the entire data set and compared them with a piecewise flow period that uses convolution to account for varying wellbore flow rates. They studied the application of the multistep test for both shut-in and producing wells. They concluded that the multistep well test can be properly analyzed only following model identification. However, they did not consider fractured reservoirs. Cobb et al[54] utilized the conventional methods of Muskat, Miller-Dyes-Hutchinson and Horner for the interpretation of pressure buildup in bounded two-layered reservoir without cross-flow. Their work confirmed that of Lefkovitz et al[7]. Sullivian et al[57] developed a constant rate drawdown type curves for analyzing pressure buildup test which follow production at

constant bottom hole flowing pressure for commingled gas reservoir containing hydraulic fractures. They determined that the multilayer solution matches the single layer solution when the dimensionless wellbore pressure is plotted as a function of $\frac{t_D}{C_{RD}{}^2}$ for finite multilayered reservoir with unequal layer areas. However, their type curves cannot be used in a general case because it is applicable to a specific type of layered reservoir. They showed that "when describing a reservoir type different from what they studied, the Engineer may find it useful to develop type curves for analysis of test from that reservoir. These type curves like the curves developed in this study can serve to help identify the reservoir type and to provide at least useful first estimation of key reservoir properties". They determined that for different values of reservoir conductivity, $C_{RD,}$ $\frac{k_1h_1}{K_2h_2}$ and dimensionless fracture conductivity, C_{fD}, a dimensionless parameter $\frac{X_f}{A_2}$ correlates P_D versus $\frac{t_D}{C_{RD}{}^2}$ graphs for widely varying values of X_f and A_2. Prijambodo et al[58] investigated the pressure response of a well producing from a two-layer reservoir with interlayer crossflow. They characterized the early time pressure behavior and suggested that interpretations of pressure buildup data based on single layer theory can lead to erroneous results, with error magnitude depending on the degree of layer communication.

Very few literature have considered fractured multilayered reservoir and none seems to consider partial penetrating fractures in multilayered reservoir. This research seeks to bridge this gap by developing equations to model both fully and partially penetrating fractures in multilayered commingled reservoirs. The properties of both the fracture and reservoir can be estimated with these analytical equations.

2.3 Types of Multilayer Reservoir

Multilayer Reservoirs can be classified into two: layered reservoir with crossflow, in which layers communicate at the contact planes and layered reservoir without crossflow, in which layers communicate only at the wellbore. This type of system without crossflow is also called commingled reservoir. These classifications are discussed below.

2.3.1 Commingle Reservoir

Here, the layers do not communicate in terms of fluid flow through the formation but may be produced by the same wellbore. The wellbore in a commingled system may be vertical, horizontal, inclined or partially penetrated. Individual layers may be homogeneous, heterogeneous or fractured and, can have different initial, inner and outer conditions, infinite extent, constant pressure, no flow or mixed. The layer (shale) between the layers is impermeable to allow fluid flow between the layers; hence the analysis involved in this type of multilayered reservoir is relatively simple as compared to crossflow multilayer and is regarded as a limiting case of a crossflow system where the vertical permeabilities of all the layers are assumed to be negligible. The interporosity layer flow parameter, λ, is consequently zero depicting the fact that no flow occurs across the layers. On the pressure derivative, a horizontal line, which is a constant during the pseudo-radial flow, can be used to estimate the average flow capacity of all the layers. The second final horizontal line (if two-layers are considered) can be used to estimate the ratio of the flow capacity of the second layer (low permeable layer) to the average flow capacity.

2.3.2 Cross-flow

The layers communicate in the formation. At early time however, cross-flow multilayered reservoir behave as though they were commingled. This is because at early time, the differential

depletion is not significant and hence the pressure differential cannot cause fluid flow from one layer to another. At late time, the differential pressure between the layers become significant and since the interlayer flow parameter is not zero, fluid flows from one layer (the lower permeable) to the other (higher permeable layer). On the pressure derivative, after the wellbore storage effect, a horizontal line is observed which depicts depletion of the higher permeable layer. Depending on the magnitude of the interlayer flow parameter, a time is reached where fluid flows from the lower permeable layer to the higher permeable layer. This is indicated as a trough on the pressure derivative. A horizontal line is finally observed depicting the total system behavior during the pseudo-radial flow.

2.4 Testing Techniques in Multilayered Reservoirs

2.4.1 Introduction

The layered reservoir Test (LRT) relies on a combination of measurements including production logs surveys, pressure and flow rate transients required with the sensors in a stationary position. Recent developments in multilayer well testing have focused on the determination of individual layer properties and, this can be achieved by measuring the wellbore pressure and the flow rate with a production logging tool as a function of time and vertical depth along the wellbore. The flow rates are measured just above the individual layers as transients are produced by altering the surface flow rates in steps. By measuring the flow rate and pressure transients beginning from the bottom layer, its properties can be estimated. The flow meter is then moved to the top of the next layer.

2.4.2 Sequential Testing

The procedure is as follows:

1. Position the production logging tool (PLT) above the bottom layer and flow the well at a constant surface rate. Record the flow rate of the bottom layer as well as the bottom hole flowing pressure. The bottom-hole flowing pressure is sensitive to the entire layers.
2. Place the flow meter above the next layer and record the flow rate.
3. Repeat the above procedure for all the layers without changing the surface flow rate.
4. Change the surface flow rate and position the PLT above the bottom layer and repeat the procedure above.
5. Pull the tool out of hole. The pressure and flow rate data can then be used to estimate the individual layer properties.

In sequential testing, one flow meter is used; hence the properties estimated are functions of the layers below it. In this regard, the parameters estimated when the flow meter was above the top of the bottom layer are true values of the bottom layer. Estimations of layers above are all averages. The parameters estimated for the bottom layer are fixed for the layer just above it which is then used to estimate the properties of the second layer. This procedure is repeated for the rest of the layers above; each time the previously determined parameters are fixed for the estimation of the properties of the next layer. Shah et al[37] have presented a detailed description and interpretation procedure of the above technique.

2.4.2.1 Disadvantages

The demerits of this technique include

1. The measurements are taken under flowing conditions and may be subject to some fluctuations in the surface flow rate
2. Measurements are also taken at different times with only one flow meter; hence superposition effects ought to be taken into consideration.
3. Also, each measurement is initiated by a change in surface flow rate of arbitrary magnitude. As a result, it is not possible to subtract the flow rates transient measurements taken at different times.

2.4.2.2 Advantages

1. It provides an approximate correction for superposition effects by using the difference between the measured transient pressure/flow rate during the flow period and the pressure/flow rate values recorded first before the flow rate change.
2. The pressure and flow rate differences can be modeled with the drawdown as long as the transient flow duration is small compared with the length of the previous rate period.

2.4.3 Commingle Single-Layer Testing (CSLT)

In this technique, two flow meter sensors are positioned such that one is just above the layer perforation and the other is below it. In this way, the difference between the flow meter readings $q_a - q_b$ is equal to the layer flow rate. Here, q_a is the flow meter reading above the layer of interest while q_b is the flow meter reading below the same layer. A pressure sensor is placed at a fixed position in the perforated interval to measure the bottom-hole flowing pressure. The individual layer flow rate as well as the wellbore pressure can then be used to estimate the layer properties. The transient response detected by the CSLT may be homogeneous, dual porosity,

fracture or radially composite depending on the lithology and near wellbore conditions.

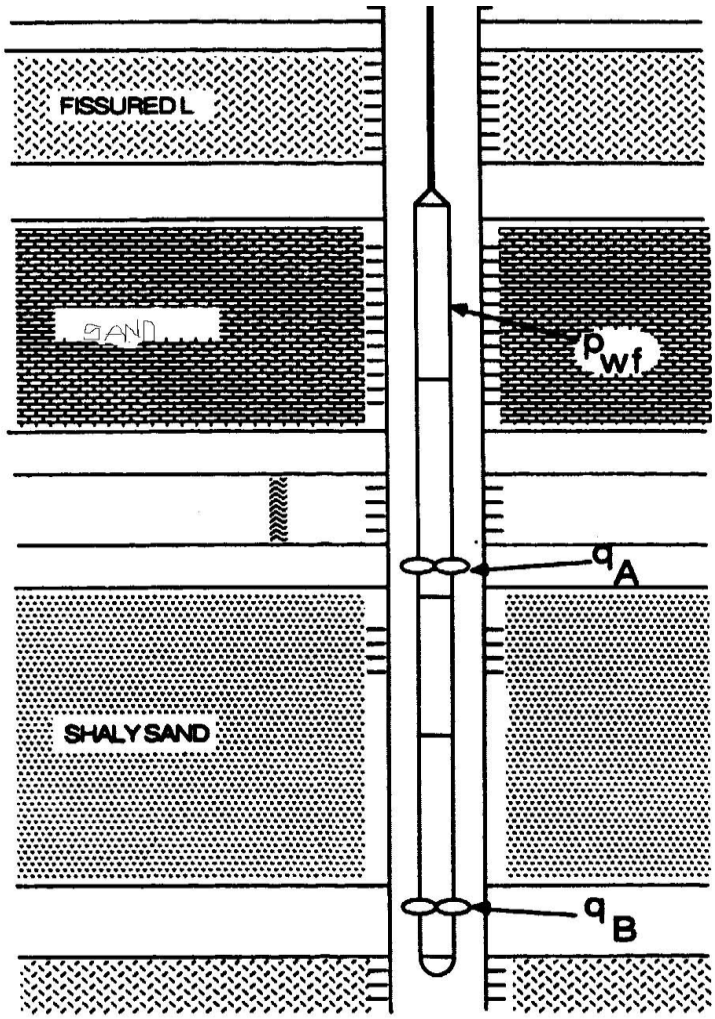

Figure 2.1: Commingle Single layer Test configuration (Source: Ehlig-Economides and Joseph[16])

The interpretation procedure is as follows:

1. Position the flow meters above and below the layer of interest while the well is flowing at a constant surface flow rate. Record the flow meters readings and wellbore pressure and, determine the stabilized trend in flow rates and pressure at the end of the flow period.
2. Change the surface flow rate and record the layer flow rate and wellbore pressure versus elapsed time, Δt, since the surface rate change.

3. Determine the flow rate, $q_L(t)$, for the layer tested both before and after the surface rate change, $q_L\ t\ = q_a(t) - q_b(t)$. If the layer is accepting fluid instead of producing, $q_L\ t\ $ will be negative.
4. Using the computed values of $q_L\ t\ $, calculate

   $\Delta q_L\ \Delta t\ = q_L(t_1) - q_L(\Delta t)$

   $\Delta P_{wf}\ \Delta t\ = P_{wf}(t_1) - P_{wf}(\Delta t)$

Where $q_L\ t_1\ and\ P_{wf}\ t_1\ $ were recorded just before the rate change at time t_1.

5. Calculate the rate normalized pressure, $\Delta P_{wf}\ \Delta t\ /\Delta q_L\ \Delta t\ $, and rate convolved time function.

2.4.3.1 Disadvantages

1. The measurements are taken under flowing conditions and may be subject to some fluctuations in the surface flow rate

2.4.3.2 Advantages

1. Superposition effect is greatly minimized since two flow meters are used at the same time. Here, a simple subtraction between the flow meter readings gives the layer flow rate at a particular time.

2. Flow rate measurement is faster as compared to the sequential technique.

2.4.4 Multi flow meter testing

Here, flow meter sensors are positioned above and below all the layers at the same time. As a result, flow rates of all the layers can be measured at a time and the same interpretation procedure as done for CSLT is carried out.

2.4.4.1 Disadvantage

1. High cost is involved since the number of flow meters require for the test is determined by the number of layers.

2.4.4.2 Advantages

1. Superposition effect is greatly minimized since individual flow rates are measured at the same time. Here, a simple subtraction between the flow meter readings gives the layer flow rate at a time.

2. Flow rate measurement is faster.

2.5 Literature summary

The testing techniques illustrated above seem to suggest that multi-rate testing is required for the analysis of multilayered reservoir. However, Gao[35] showed that the individual layer properties of a multilayer reservoir with or without crossflow can be determined by one drawdown test if all the layers are tested together and the common wellbore pressure and the flow rate for each layer are measured and analyzed. Hence, a single test can also be used for the estimation of layered properties. Usually, the first flow rate is used to determine the producing layers so as to ascertain which layer is productive after which the individual layer properties estimation is carried out with the second flow test. Additionally, most of the previous literatures have concentrated on

unfractured layered reservoir and very few have considered fractured layered reservoir, but none, to my knowledge, has considered partially penetrating fracture in layered reservoir. Modeling a layer that has been partially fractured in multilayered reservoir has not been considered in the literature.

CHAPTER 3 MATHEMATICAL FORMULATION

3.1 Model Description

The physical model discussed in this work is a multilayered reservoir that is being drained by a hydraulically fractured well. The layers communicate only at the wellbore and there is no interlayer cross-flow. Each layer may be fully fractured as shown in figure 2 and the properties of each fracture in each layer may be different from that of other layers. The fracture may also be partially penetrating such that the height of the fracture becomes less than the height of the layer as depicted by figure 3. One or more layers may not be fractured at all.

Additional assumptions made in this work include

- Each layer is assumed to be homogeneous, isotropic but has distinct properties from other layers
- At t=0,the pressure is uniform throughout the reservoir
- Gravity effects are negligible. (Pressure gradients are small).
- The reservoir produces at constant surface rate
- The fractured layers are in communication with the wellbore only by means of the fractures and there is no cross flow between layers
- Both the fractures and the reservoir are filled with a single, slightly compressible fluid of constant viscosity
- The reservoir is infinite in extent and is impermeable both at the upper and lower boundaries

- The well is symmetrically located and penetrates the entire layers

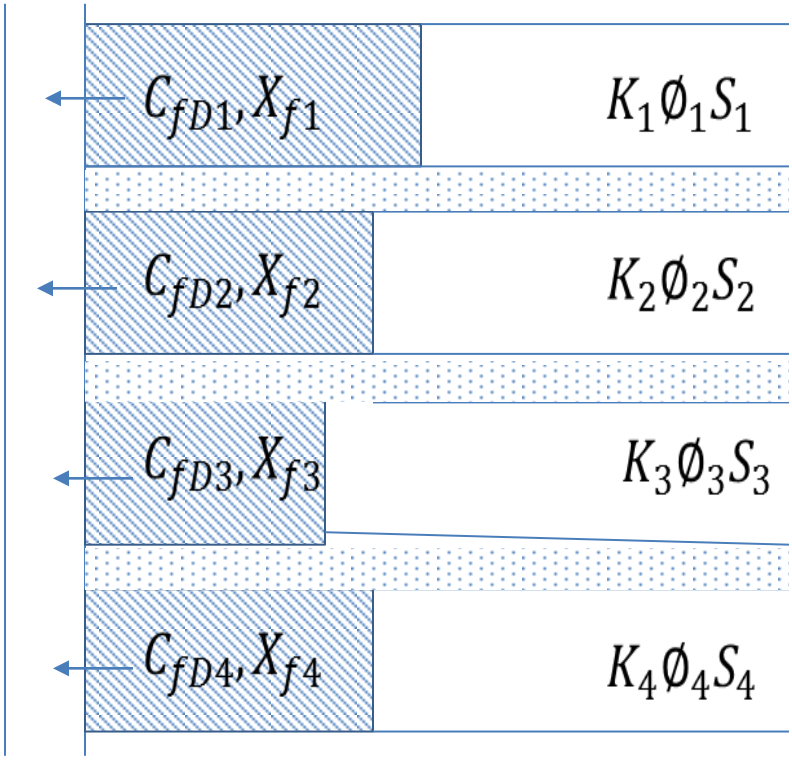

Figure 3.1: Fully fractured commingled multilayered reservoir

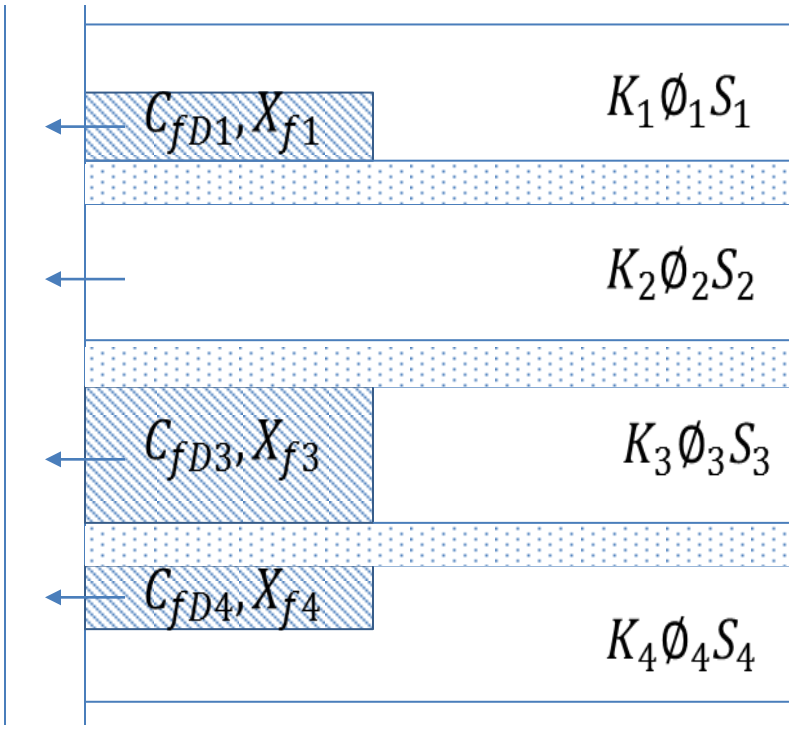

Figure 3.2: Partially penetrating fractured commingled multilayered reservoir

3.2 **Pressure and Pressure Derivative Analysis**

Definition of terms

$$P_{WD} = \frac{Kh\ \ P_i - P_{wf}(t)}{141.2q\mu B} \tag{3.2.1}$$

$$\frac{1}{q_D} = \frac{Kh\ \ P_i - P_{wf}}{141.2q(t)\mu B} \tag{3.2.2}$$

$$t_{Dx_f} = \frac{0.0002637K}{\emptyset\mu C_t X_f^2} t \tag{3.2.3}$$

$$C_{fD} = \frac{K_f w_f}{K X_f} \tag{3.2.4}$$

$$S_{fD} = \frac{\emptyset_f C_{ft} w_f}{\emptyset C_t X_f} \tag{3.2.5}$$

$$\eta_{Dj} = \frac{\eta_j}{\eta} \tag{3.2.6}$$

$$\eta = \frac{k}{\emptyset C_t \mu} \tag{3.2.7}$$

$$\eta_j = \frac{k_j}{\emptyset_{tj} C_{tj} \mu} \tag{3.2.8}$$

$$k = \frac{1}{h} \sum_{j=1}^{n} k_j\, h_j \tag{3.2.9}$$

$$\emptyset C_t = \frac{1}{h} \sum_{j=1}^{n} \emptyset_j\, C_{tj} h_j \tag{3.2.10}$$

$$h_{fD} = \frac{h_f}{h} \tag{3.2.11}$$

$$R_{cDj} = \frac{k_j h_j}{kh} \quad \frac{1}{\overline{\eta_{Dj}}} \tag{3.2.12}$$

$$R_{cD} = \frac{1}{kh} \sum_{j=1}^{n} k_j h_j \quad \frac{1}{\eta_{Dj}} \quad = \sum_{j=1}^{n} R_{cDj} \tag{3.2.13}$$

The dimensionless wellbore pressure for a fractured well in a commingled reservoir is given by Bennett et al[1]

$$P_{WD} \quad t_{Dx_f} \quad = \frac{2}{h_{fD}} \quad \overline{\frac{\pi t_{Dx_f}}{C_{fD} S_{fD}}} \quad 1 + \frac{\overline{\pi}}{2} \sum_{n=1}^{\infty} b_n^{-1\ 2} \quad \frac{2R_{CD}}{h_{fD} C_{fD}} \quad ^{n} \frac{t_{D_{xf}}^{n\ 2}}{\Gamma \quad n+3 \quad 2} \tag{3.2.14}$$

where

$$b_n^{-1\ 2} = \frac{-1 \quad 2 \quad -3 \quad 2 \quad \ldots\ldots \quad 1 \quad 2 - n}{n!} \tag{3.2.15}$$

for n >1or =1; and $b_0^{-1\ 2} = 1 \quad 2$

3.2.1 Fracture linear flow (Masked by Wellbore storage effect)

At very short time, the flow of fluid to the well is as a result of expansion of the fluid within the fracture. For very small time, equation (3.2.14) yields Bennett et al[1]

$$P_{WD} \quad t_{Dx_f} \quad = \frac{2}{h_{fD}} \quad \overline{\frac{\pi t_{Dx_f}}{C_{fD} S_{fD}}} \tag{3.2.16}$$

The above equation is similar to Cinco Ley et al[4] for single layer flow. Though equation (3.2.16) is masked by wellbore storage effect and is not observed practically, it shows that at very early time, the dimensionless wellbore pressure is influenced by the fracture property (C_{fD}, S_{fD}) and not the formation.

Fully penetrating fractures:

3.2.2 Bilinear flow regime

At early time, when the fracture tip effects is not felt at the wellbore, fluid flows linearly and perpendicularly to the fracture face and linearly within the fracture. The dimensionless wellbore pressure in a fully fractured commingled reservoir is given by Bennett et al[1]

$$P_{WD} = 2.45\ \frac{t_{Dx_f}\ \ R_{CD}^{\ 2}}{C_{fD}^{\ 2}}^{\ 1\ 4} \qquad (3.2.2.1)$$

For homogenous reservoir R_{CD}= 1and equation (3.2.2.1) becomes similar to Cinco Ley and Samaniego[4] equation for single layer reservoir.

Now, substituting the dimensionless variables into equation (3.2.2.1) yields

$$\Delta P = \frac{44.13qB\mu}{h\ \ \overline{K_f W_f}\ \ R_{CD}^{\ 1\ 2}\ \ \emptyset\mu C_t K^{\ 1\ 4}}\, t^{\ 1\ 4} \qquad (3.2.2.2)$$

The dimensionless reservoir conductivity $R_{CD,}$ is determined by core analysis Bennett et al[1] and is 1 for homogeneous single layer and less than 1 for heterogonous layers.

Now, Let

$$m_{BL} = \frac{44.13qB\mu}{h\ \ \overline{K_f W_f}\ \ R_{CD}^{\ 1\ 2}\ \ \emptyset\mu C_t K^{\ 1\ 4}} \qquad 3.2.2.3$$

Equation (3.2.2.2) becomes

Hence, $\Delta P = m_{BL} t^{0.25}$ (3.2.2.4)

Taking the logarithm of both sides of equation (3.2.2.4) yields

$$\log \Delta P = \log m_{BL} + \frac{1}{4}\log t \qquad (3.2.2.5)$$

Equation (3.2.2.5) shows that a log-log plot of ΔP versus t yields a straight line of slope 0.25, which is a unique characteristic of bilinear flow.

At t=1hr;

$(\Delta P)_{BL1} = m_{BL}$ (3.2.2.6), which can be used with equation (3.2.2.3) to estimate the fracture conductivity as follows:

$$K_f W_f = \frac{1947.46}{R_{CD}\sqrt{\emptyset \mu C_t K}} \left(\frac{q\mu B}{h(\Delta P)_{BL1}}\right)^2 \qquad (3.2.2.7)$$

For a single layer reservoir, R_{CD}=1 and equation (3.2.2.7) reduces to what Tiab[5] derived (see ref 5 eqn 6 if ω=1 for homogeneous reservoir).

Now taking the derivative of equation (3.2.2.1) with respect to time yields

$$P'_{WD} * t_{Dx_f} = \frac{0.6127}{R_{CD}\sqrt{C_{fD}}} t_{Dx_f}^{0.25} \qquad (3.2.2.8)$$

This equation is again similar to what Tiab derived for single homogeneous layer ($R_{CD} = 1$)

Substituting the dimensionless variables into equation (3.2.2.8) yields

$$\Delta P' * t = 0.25 m_{BL}\, t^{1/4} \qquad (3.2.2.9)$$

Taking logarithm of both sides of equation (3.2.2.9) yields

$$\log\ \Delta P' * t\ = 0.25\log t + \log\ 0.25 m_{BL} \qquad (3.2.2.10)$$

Equation (3.2.2.10) also shows that a log-log plot of $\Delta P' * t$ versus t yields a straight line of slope 0.25, which is a unique characteristic of bilinear flow.

At t=1hour, equation (3.2.2.10) becomes

$$\Delta P' * t\ _{BL1} = 0.25 m_{BL} \qquad (3.2.2.11)$$

Now, comparing equation (3.2.2.11) and (3.2.2.9), at t =1 hour;

$$\Delta P' * t\ _{BL1} = 0.25\ \Delta P\ _{L1} \qquad (3.2.2.12)$$

The fracture conductivity is computed using equation (3.2.2.11) as

$$W_f k_f = \frac{121.74}{R_{CD}\ \sqrt{\emptyset \mu C_t K}}\ \frac{q\mu B}{h\ \Delta P' * t\ _{BL1}}^{\ 2} \qquad (3.2.2.13)$$

Tiab has shown that the fracture conductivity, in the absence of the bilinear flow regime, can be estimated as

$$W_f k_f = \frac{1.92173}{\frac{1}{r_w'} - \frac{3.31739k}{X_f}} \qquad (3.2.2.14)$$

Equations (3.2.2.13) and (3.2.2.14) give the estimated average fracture conductivity of the entire fractured layers and do not yield the fracture conductivity of each layer. This is because the bottom-hole flowing pressure is sensitive to the total system

It is observed that the introduction of the dimensionless reservoir conductivity, R_{CD}, into equation (3.2.2.13) distinguishes a multilayered reservoir from single layered reservoirs.

3.2.3 Formation Linear flow

When the fracture tip effect is felt at the wellbore, the flow in the formation is parallel to the fracture face. The dimensionless wellbore pressure in a fully fractured commingled reservoir is given by Bennett et al[1],

$$P_{WD} = \frac{1}{R_{CD}} \quad \overline{\pi t_{Dx_f}} \tag{3.2.3.1}$$

Substituting the dimensionless variables into equation (3.2.3.1) yields

$$\Delta P = \frac{4.064qB}{hR_{CD}} \quad \overline{\frac{\mu}{K\emptyset C_t X_f^2}}\ t^{0.5} \tag{3.2.3.2}$$

Let

$$m_L = \frac{4.064qB}{hR_{CD}} \quad \overline{\frac{\mu}{K\emptyset C_t X_f^2}} \tag{3.2.3.3}$$

Hence, from equation (3.2.3.2)

$$\Delta P = m_L t^{0.5} \tag{3.2.3.4}$$

Taking the logarithm of both sides of equation (3.2.3.4) yields

$$\log \Delta P = \log m_L + 0.5 \log t \tag{3.2.3.5}$$

A slope of 0.5 is obtained from equation (3.2.3.5), which is a unique characteristic of a linear flow regime.

At t=1hour, equation (3.2.3.5) becomes

$(\Delta P)_{L1} = m_L$ …(3.2.3.6), which can be used with equation (3.2.3.3) to estimate the fracture half length as follows:

$$X_f = \frac{4.064qB}{hR_{CD}(\Delta P)_{L1}} \quad \overline{\frac{\mu}{K\emptyset C_t}} \tag{3.2.3.7}$$

Now taking the derivative of equation (3.2.3.1)

$$P'_{WD} * t_{Dx_f} = \frac{1}{2R_{CD}} \quad \overline{\pi} \; t_{Dx_f}{}^{0.5} \tag{3.2.3.8}$$

Substituting the dimensionless variables into equation (3.2.38) yields

$$\Delta P' * t \; = \frac{2.032qB}{hR_{CD}} \quad \overline{\frac{\mu}{K\emptyset C_t X_f^2}} \; t^{0.5} \tag{3.2.3.9}$$

Let

$$m_L = \frac{2.032qB}{hR_{CD}} \quad \overline{\frac{\mu}{K\emptyset C_t X_f^2}} \tag{3.2.3.10}$$

Again, R_{CD} depicts a layered reservoir in equation (3.2.3.10)

Substituting equation (3.2.3.10) into (3.2.3.9) and taking logarithm of both sides of the result yields,

$$\log \; \Delta P' * t \; = 0.5\log t + \log m_L \tag{3.2.3.11}$$

A slope of 0.5 is obtained indicative of a linear flow.

The fracture half length is given by, at t = 1hr

$$X_f = \frac{2.032qB}{hR_{CD}\ \Delta P' * t\ _{BL1}}\ \sqrt{\frac{\mu}{K\emptyset C_t}} \qquad (3.2.3.12)$$

Tiab has shown that the half fracture length, in the absence of the linear flow regime, can be estimated as

$$X_f = \frac{1.92173}{\frac{1}{r_w'} - \frac{3.31739k}{W_f k_f}} \qquad (3.2.3.13)$$

Equations (3.2.3.12) and (3.2.3.13) give the estimated average half fracture length of the entire fractured layers and do not yield the fracture half length of each layer. This is because the bottom-hole flowing pressure is sensitive to the total system

3.2.4 Pseudo-radial flow

During this flow regime, fluid flows radially in both fractured and unfractured layers, hence the radial diffusivity can be used to model such a reservoir.

$$P_{Dj} = \frac{K\mathrm{h}\ P_i - P_j}{141.2\mathrm{q}\mu\mathrm{B}} \qquad (3.2.4.1)$$

$$\eta_{Dj} = \frac{\eta_j}{\eta} \qquad (3.2.4.2)$$

$$\eta = \frac{k}{\emptyset C_t \mu} \qquad (3.2.4.3)$$

$$\eta_j = \frac{k_j}{\emptyset_{tj} C_{tj} \mu} \qquad (3.2.4.4)$$

$$t_{Dx_f} = \frac{0.0002637K}{\emptyset \mu C_t X_f^2} t \qquad (3.2.4.5)$$

if all the layers are fractured

$$t_{Dx_f} = \frac{0.0002637K}{\emptyset \mu C_t X_f^2} t + \frac{0.0002637k}{\emptyset \mu C_t r_w^2} t \qquad (3.2.4.6)$$

for two layered reservoir of which one is fractured.

J.L. Johnston and W.J. Lee[8] have shown that the layer dimensionless pressure (also shown in appendix A) during the pseudo-radial flow in commingled reservoir is given by

$$P_{Dj} = \frac{K_O \; r_D f(u_j)}{u} \tag{3.2.4.7}$$

$f(u_j)$ reflects the heterogeneity of the reservoir; since each layer is homogeneous (but have different properties from other layers);

$$f \; u_j \; = \; \overline{u_j} \tag{3.2.4.8}$$

Hence, equation (3.2.4.7) becomes

$$P_{Dj} = \frac{K_O \; r_D \; \overline{u_j}}{u} \tag{3.2.4.9}$$

Upon inversion,

$$P_{Dj} = -\frac{1}{2} \; E_i \; -\frac{r_D^2}{4t_{Dxf}} \tag{3.2.4.10}$$

P_{Dj} is the dimensionless pressure of layer j.

Equation (3.2.4.11) is the line source solution of layer j in commingle reservoir.

At the wellbore $r_D = 1$, and equation (3.2.4.10) reduces to

$$P_{WD} = -\frac{1}{2} \; E_i \; \frac{1}{4t_D} \tag{3.2.4.11}$$

The logarithmic approximation to equation (3.2.4.11) during the pseudo-radial flow is

$$P_{WD} = 0.5 \; lnt_D + 0.80907 + 2S \tag{3.2.4.12}$$

Substituting the dimensionless variables yields into equation (3.2.4.12)

$$\frac{kh\Delta P}{141.2q\mu B} = \frac{1}{2} \; \ln t + \ln \frac{k}{\emptyset \mu C_t r_w^2} - 7.43 + 2s \tag{3.2.4.13}$$

$$\Delta P = \frac{70.6q\mu B}{kh} \; \ln t + \ln \frac{k}{\emptyset \mu C_t r_w^2} - 7.43 + 2s \tag{3.2.4.14}$$

Differentiating equation (3.2.4.14) with respect to $\ln t$ yields

$$\frac{d\Delta P}{d\ln t} = \Delta P' * t = \frac{70.6q\mu B}{kh} \qquad (3.2.4.15)$$

Hence, during the radial flow regime, a constant which is a horizontal line on the derivative is developed. The average permeability is computed as

$$K = \frac{70.6q\mu B}{h\ \Delta P' * t\ _r} \qquad (3.2.4.16)$$

Now, substituting (3.2.4.15) into (3.2.4.13) and making the skin the subject

$$s = 0.5\ \frac{(\Delta P)_r}{t * \Delta P'\ _r} - \ln\frac{Kt_r}{\emptyset\mu C_t {r_w}^2} + 7.43 \qquad (3.2.4.17)$$

3.3 Rate and Rate Derivative Analysis

Pressure data are influenced by wellbore storage effects at early time. These effects prohibit a good formation description of the area at the vicinity of the wellbore (Nashawi and Mallalah[40]). It is reasonable to use the reciprocal rate and rate derivative analysis for wells producing at constant bottom hole flowing pressure for average multilayer reservoir parameter estimation.

3.3.1 Bilinear flow

The constant bottom-hole flowing pressure equation governing the flow in a commingled fractured reservoir during the bilinear flow regime in the dimensionless form is given by Bennett et al[1],

$$P_{WD} = \frac{1}{q_D} = 2.45\ \frac{t_{Dx_f}\quad {R_{CD}}^{\ 2}}{{C_{fD}}^{\ 2}}^{\ 1\ 4} \qquad (3.3.1.1)$$

The dimensionless reservoir conductivity is determined by core analysis (Bennett et al[1]) and is 1 for homogeneous single layer and less than one for heterogonous layers.

Now, substituting the dimensionless variable into equation (3.3.1.1) yields

$$\frac{1}{q(t)} = \frac{44.13B\mu}{h\Delta P \quad \overline{K_f W_f R_{cD}}^{\,1\,2} \; \emptyset\mu C_t K^{\,1\,4}} t^{1\,4} \qquad (3.3.1.2)$$

Let

$$m_{BL} = \frac{44.13B\mu}{h_j\Delta P \quad \overline{K_f W_f} \; R_{CD}^{\,1\,2} \; \emptyset\mu C_t K^{\,1\,4}} t^{1\,4} \qquad (3.3.1.3)$$

Hence, equation (3.3.1.2) becomes

$$\frac{1}{q(t)} = m_{BL} t^{0.25} \qquad (3.3.1.4)$$

Taking the logarithm of both sides of equation (3.3.1.4) yields

$$\log\frac{1}{q(t)} = \log m_{BL} + \frac{1}{4}\log t \qquad (3.3.1.5)$$

Equation (3.3.1.5) shows that a log-log plot of $\frac{1}{q(t)}$ versus t yields a straight line of slope 0.25, which is a unique characteristic of bilinear flow.

At t=1hr; equation (3.3.1.5) becomes

$\frac{1}{q}_{BL1} = m_{BL}$ (3.3.1.6), which can be used with equation (3.3.1.3) to estimate the fracture conductivity as follows:

$$K_f W_f = \frac{1947.46}{R_{CD}\ \overline{\emptyset \mu C_t K}}\ \left(\frac{\mu B}{h \Delta P\ \frac{1}{q}_{BL1}}\right)^2 \qquad (3.3.1.7)$$

For a single layer reservoir, R_{CD}=1 and equation (3.3.1.7) reduces to what Tiab[11] derived (if ω=1 for homogeneous reservoir).

Now taking the derivative of equation (3.3.1.4) yields

$$-\frac{1}{q^2}\ \Delta q' * t\ = 0.25 m_{BL} t^{0.25} \qquad (3.3.1.5)$$

Now, taking the logarithm of both sides of equation (3.3.1.5) yields

$$\log\ -\frac{1}{q^2}\ \Delta q' * t\ = 0.25 \log t + \log\ 0.25 m_{BL} \qquad (3.3.1.6)$$

Equation (3.3.1.7) shows that a log-log plot of $-\frac{1}{q^2}\ \Delta q' * t$ versus t yields a straight line of slope 0.25, which is a unique characteristic of bilinear flow. Usually, the derivative is more sensitive to rate variations than the rate and hence it is important to plot both plots so as to identify the correct location of the derivative plot.

The rate and rate derivative relationship can be computed as follows:

At t=1hour, equation (3.3.1.6) becomes

$$-\frac{1}{q^2}\ \Delta q' * t\ _{BL1} = 0.25 m_{BL1} \qquad (3.3.1.7)$$

Now, comparing equation (3.3.1.7) and (3.3.1.5), at t =1 hour;

$$-\frac{1}{q^2}\ \Delta q' * t\ _{BL1} = 0.25\ \frac{1}{q}\ _{BL1} \tag{3.3.1.7}$$

The fracture conductivity is computed using equation (3.3.1.7) as

$$K_f W_f = \frac{121.74}{R_{CD}\ \sqrt{\emptyset\mu C_t K}}\ \frac{\mu B}{h\Delta P\ -\frac{1}{q^2}\ \Delta q' * t\ _{BL1}} \tag{3.3.1.8}$$

It is observed that the introduction of the dimensionless reservoir conductivity, R_{CD}, into equation (3.3.1.8) distinguishes a multilayered reservoir from single layered reservoirs.

3.3.2 Formation Linear flow

When the fracture tip effect is felt at the wellbore, the flow in the formation is parallel to the fracture face. The constant bottom-hole flowing pressure equation governing the flow in a commingled fully fractured reservoir during the linear flow regime in the dimensionless form is given by Bennett et al[1],

$$P_{WD} = \frac{1}{q_D} = \frac{1}{R_{CDj}}\ \sqrt{\pi t_{Dx_f}} \tag{3.3.2.1}$$

Substituting the dimensionless variables into equation (3.3.2.1) yields

$$\frac{1}{q} = \frac{4.064B}{h\ \ \Delta P\ (R_{CD})}\ \sqrt{\frac{\mu}{k\emptyset C_t X_f^2}}\ t^{0.5} \tag{3.3.2.2}$$

Let

$$m_L = \frac{4.064B}{h \quad \Delta P \ (R_{CD})} \quad \sqrt{\frac{\mu}{k\emptyset C_t X_f^2}} \tag{3.3.2.3}$$

Hence, equation (3.3.2.3) becomes

$$\frac{1}{q} = m_L t^{0.5} \tag{3.3.2.4}$$

Taking the logarithm of both sides of equation (3.3.2.4) yields

$$\log\frac{1}{q} = \log m_L + 0.5\log t \tag{3.3.2.5}$$

Equation (3.3.2.5) shows that a log-log plot of $\frac{1}{q}$ versus t yields a straight line of slope 0.5, which is a unique characteristic of linear flow.

At t=1hour, equation (3.3.2.5) becomes

$\frac{1}{q}_{L1} = m_{L1}$ ……(3.3.2.6), which can be used with equation (3.3.2.3) to estimate the fracture half length as follows:

$$X_f = \frac{4.064qB}{\frac{1}{q}_{L1}(h)(R_{CD})(\Delta P)} \quad \sqrt{\frac{\mu}{k\emptyset C_t}} \tag{3.3.2.7}$$

Now taking the derivative of equation (3.3.2.4) yields

$$-\frac{1}{q^2} \ \Delta q' * t \ = 0.5 m_L t^{0.5} \tag{3.3.2.8}$$

Taking the logarithm of both sides of equation (3.3.2.8) yields

$$\log \ -\frac{1}{q^2}\ \Delta q' * t \ \ = 0.5\log t + \log(\ 0.5m_L) \qquad (3.3.2.9)$$

Equation (3.3.2.9) shows that a log-log plot of $-\frac{1}{q^2}\ \Delta q' * t$ versus t yields a straight line of slope 0.5, which is a unique characteristic of linear flow.

At t=1hour; equation (3.3.2.9) becomes

$$-\frac{1}{q^2}\ \Delta q' * t \ \ _{L1} = 0.5m_L \qquad (3.3.2.10))$$

Hence, the fracture half length is given by, at t = 1hr,

$$X_f = \frac{2.032qB}{h(R_{CD})(\Delta P)\ \ -\frac{1}{q^2}\ \Delta q' * t \ \ _{L1}}\ \ \overline{\frac{\mu}{K\emptyset C_t}} \qquad (3.3.2.11)$$

3.3.3 Pseudo-radial flow

The equation governing pseudo-radial flow for constant flow rate is given by

$$P_{WD} = \frac{1}{q_D} = 0.5\ \ lnt_D + 0.80907 + 2S \qquad (3.3.3.1)$$

Substituting the dimensionless variables into equation (3.3.3.1) yields

$$\frac{1}{q} = \frac{70.6B\mu}{Kh\Delta P}\ \ln\ \ \frac{0.0002637Kt}{\emptyset\mu C_t r_w^2}\ \ + 0.80907 + 2S \qquad (3.3.3.2)$$

Taking the derivative of equation (3.3.3.2) with respect to t yields

$$-\frac{1}{q^2}\ \Delta q' * t\ _r = \frac{70.6B\mu}{Kh\Delta P} \quad (3.3.3.3)$$

Hence, during the pseudo-radial flow, this constant, which is a horizontal line on the derivative, is observed. The average permeability can then be determined as

$$K = \frac{70.6B\mu}{h\Delta P\ \ -\frac{1}{q^2}\ \Delta q' * t\ _r} \quad (3.3.3.4)$$

The skin can be calculated as follows:

Substituting equation (3.3.3.3) into equation (3.3.3.2) and making S the subject yields

$$S = 0.5\ \frac{^1 q\ _r}{-\frac{1}{q^2}\ \Delta q' * t\ _r} - \ln\ \frac{Kt_r}{\emptyset\mu C_t r_w^2}\ + 7.43 \quad (3.3.3.5)$$

t_r is any convenient time taken from the horizontal line corresponding to the pseudo-radial flow regime, $^1 q\ _r\ and\ -\frac{1}{q^2}\ \Delta q' * t\ _r$ are the corresponding or matching values on the reciprocal rate and derivative respectively.

3.4 Rate Normalized Pressure and Rate Normalized Pressure Derivative Analysis

In order to estimate the properties of the individual layers, down-hole flow rate and wellbore pressure are needed. For commingle reservoir, the pressure at the wellbore is defined by the convolution integral Gao et al[20] as:

$$\Delta P_{wf}\ t\ = \frac{Kh}{K_j h_j}\ \int_0^t q_{sfD}\Delta P'_{sf}\ t-\tau\ d\tau \quad (3.4.1)$$

For a single layer,

$$\frac{Kh}{K_j h_j} = 1$$

$\Delta P_w\ t$ is the wellbore pressure drop due to varying flow rate

q_{sfD} is the dimensionless (or normalized) sandface rate and is given by

$$q_{sfD} = \frac{q_{sf}}{q_{ref}} \tag{3.4.2}$$

Where q_{ref} is the reference rate, which is the total rate from all the layers. In multilayered testing, the flow meter(s) is/are located above the layer of interest and not at the perforations, hence in this thesis, the measured flow rate, qm, will be used to distinguish it from sandface flow rate, qsf, which is that at the perforations. This is because the wellbore storage effect will be due to the fluid volume below the flow meter.

$$\Delta P'_{sf} = \Delta P'_f\ t\ + \Delta P_s \tag{3.4.3}$$

$\Delta P'_f$ is the derivative of the pressure drop at the sandface if the flow rate had been constant

Hence $\Delta P'_{sf}$ is the impulse function.

Now equation (3.4.1) can be rewritten as:

$$\Delta P_{wf}\ t\ = \frac{Kh}{K_j h_j} \int_0^t q_{mDj} \Delta P'_{wcf}\ t - \tau\ d\tau \tag{3.4.4}$$

In dimensionless form, equation (3.4.4) becomes

$$P_{wD}\ t\ = \frac{Kh}{K_j h_j} \int_0^t q_{mDj} \frac{dP_{wcD}\ t-\tau}{d\tau_D} d\,\tau_D \qquad (3.4.5)$$

The flow rate and pressure are measured at discrete intervals of time; hence the integral relationship given in equation (3.4.5) can be readily evaluated as a summation of discrete intervals of time for which the flow rate history is assumed to be piecewise continuous, as a series of constant flow rate steps to yield

$$P_{wD}\ t\ = \frac{Kh}{K_j h_j} \sum_{i=1}^{n} q_{mDi} - q_{mDi-1}\ \ P_{wcD}\ t_D - t_{Di-1} \qquad (3.4.6)$$

$$q_{mDj}\ t_D = 0\ \ = 0 \qquad (3.4.7)$$

$$q_{mDj} = \frac{q_{mj}}{q_{ref}} \qquad (3.4.8)$$

3.4.1 Logarithmic Convolution

Here, the logarithmic convolution which assumes a radial model is applied. Permeability and skin of each layer will be estimated here.

Now during the infinite acting radial flow, the influence function is approximated by the log approximation as:

$$P_{wcD} = 0.5\ lnt_D + 0.80907 + 2s \qquad (3.4.1.1)$$

$$P_{wcD} = 1.1513\ \log t + b \qquad 3.4.1.2$$

Where

$$\mathrm{b} = \log \frac{K}{\emptyset \mu C_t X_f^2} - 3.227 + 0.868s \qquad (3.4.1.3)$$

Now, substituting equation (3.4.1.2) into equation (3.4.6) yields

$$P_{wD} = 1.1513 \frac{Kh}{K_j h_j} \sum_{i=1}^{n} q_{Di} - q_{Di-1} \ \log\ t - t_{i-1} \ + b \qquad (3.4.1.4)$$

Substituting for dimensionless pressure yields

$$\frac{P_i - P_{wf}(t)}{\Delta q_{mj}(t)} = \frac{162.6\mu B}{K_j h_j} \sum_{i=1}^{n} \frac{q_i - q_{i-1}}{q_{ref}} \ \log\ t - t_{i-1} \ + b \qquad (3.4.1.5)$$

Let

$J_{wJ} = \frac{P_i - P_{wf}(t)}{\Delta q_{mj}(t)}$ (3.4.1.6) *depicts the rate normalized pressure* and

$$F_{lc} \ or \ RCTF \ = \sum_{i=1}^{n} \frac{q_i - q_{i-1}}{q_{ref}} \ \log\ t - t_{i-1} \qquad (3.4.1.7)$$

Cartesian Analysis:

Equation (3.4.1.5) can be rewritten as

$$J_{wJ} = m \ F_{lc} + b \qquad (3.4.1.8)$$

Equation (3.4.1.7) is the logarithmic convolution time function (F_{lc}) . A plot of J_{wj} versus F_{lc} yields a straight line during the radial flow of slope, $m = \frac{162.6\mu B}{K_j h_j}$ of which the layer permeability can be estimated as $K_j = \frac{162.6\mu B}{m h_j}$ and the intercept at $F_{lc} = 0$ is $R = bm$. Hence, R is simply $J_{wj}(F_{lc} = 0)$

Now, the layer skin can be estimated as

$$s_j = 1.1513\ \frac{J_{wj}(F_{lc}=0)}{m} - \log\frac{K_j}{\emptyset\mu C_t X_f^2} + 3.227 \qquad (3.4.1.9)$$

Semilog Analysis

Let

$t_{eq} = 10^{F_{lc}}$, then $\log t_{eq} = F_{lc}$, equation (3.4.1.8) can be rewritten as

$$\frac{P_i - P_{wf}(t)}{\Delta q_{mj}(t)} = m \log t_{eq} + R \qquad (3.4.1.10)$$

At $t_{eq} = 1\ hr$, equation (3.4.1.10) reduces to

$$J_{Wj}\ \ t_{eq} = 1\ \ = R = mb \qquad (3.4.1.11)$$

Rearranging the above equation and substituting for b yields the layer skin as

$$s_j = 1.1513\ \frac{J_{Wj}\ \ t_{eq} = 1}{m} - \log\frac{K_j}{\emptyset\mu C_t X_f^2} + 3.227 \qquad (3.4.1.12)$$

Extending to Tiab's Direct Synthesis

Recalling equation (3.4.1.10)

$$J_{Wj} = m \log t_{eq} + mb$$

But $\ln 10 \log x = \ln x$

Hence, multiplying $\ln 10$ through equation (3.4.1.10) yields

$$J_{Wj} \ln 10 = m\ \ \ln t_{eq} + b \ln 10 \qquad (3.4.1.13)$$

Taking the derivative of equation (3.4.1.13) with respect to $\ln t_{eq}$ yields

$$\frac{dJ_{wj}}{d\ln t_{eq}} = J'_{wj} * t_{eq} = \frac{m}{\ln 10} \quad (3.4.1.14)$$

Substituting $m = \frac{162.6\mu B}{K_j h_j}$ into equation (3.3.1.14) yields

$$\frac{dJ_{wj}}{d\ln t_{eq}} = J'_{wj} * t_{eq} = \frac{70.6\mu B}{K_j h_j} \quad (3.4.1.15)$$

Hence, the permeability of layer j

$$K_j = \frac{70.6\mu B}{h_j(t_{eq} * J'_{Wj})} \quad (3.4.1.16)$$

Now, substituting equation (3.4.1.14) into (3.4.1.13) yields

$$J_{Wj}\ln 10 = \quad J'_{wj} * t_{eq} \quad \ln 10 \quad \ln t_{eq} + b\ln 10 \quad (3.4.1.17)$$

We now have,

$$\frac{J_{wj}}{J'_{wj} * t_{eq}} - \ln t_{eq} = b\ln 10 \quad (3.4.1.18)$$

Substituting the expression for b from equation (3.4.1.3) into Equation (3.4.1.18) yields

$$\frac{J_{wj}}{J_{wj} * t_{eq}} - \ln t_{eq} = \quad \log\frac{K}{\emptyset\mu C_t X_f^2} - 3.227 + 0.868s \quad \ln 10 \quad (3.4.1.19)$$

We now have,

$$\frac{J_{wj}}{J_{wj} * t_{eq}} - \ln t_{eq} = \ln\frac{K}{\emptyset\mu C_t X_f^2} - 7.43 + 2s \quad (3.4.1.20)$$

And finally, making the layer skin, s, the subject

$$s_j = 0.5\ \frac{J_{Wj\ r}}{t_{eq} * J'_{Wj\ r}} - \ln\ \frac{K_j t_{eq_r}}{\emptyset_j \mu C_t r_w^2}\ + 7.43 \qquad (3.4.1.21)$$

3.4.2 Fully fractured layers

For fully fractured layers, the flow regime at early time will exhibit bilinear and/or linear flow. Hence assumption of radial flow and subsequent application of logarithmic convolution is erroneous. Additionally, the estimation of the fracture properties in each layer cannot be estimated with the logarithmic convolution model.

3.4.2.1 Bilinear flow

To account for the bilinear flow and subsequent estimation of fracture conductivity, it is reasonable to assume the equation relating the dimensionless wellbore pressure at constant flow rate during bilinear flow and substitute it into the dimensionless wellbore pressure of commingle reservoir.

Assuming the flow regime in layer j is bilinear; then we have, as shown by Cinco-Ley and Samaniego[4] as

$$P_{wcD} = \frac{2.45}{C_{fDj}} t_{Dxf}^{\frac{1}{4}} \qquad (3.4.2.1.1)$$

Substituting for dimensionless variables on the right hand side only yields

$$P_{wcD} = \frac{0.312 K_j^{\frac{3}{4}}}{K_f W_{f\ j}^{\frac{1}{2}}} t^{\frac{1}{4}} \qquad (3.4.2.1.2)$$

Equation (3.4.2.1.2) can be rewritten in the discretized form as

$$P_{wcD}\ t_{Di} - t_{Di-1} = \frac{0.312K_j^{\ 3\ 4}}{\emptyset_j \mu C_t^{\ 1\ 4}\ K_f W_{f\ j}^{\ 1\ 2}}\ t_n - t_{i-1}^{\ 1\ 4} \qquad (3.4.2.1.3)$$

Now recalling equation (3.4.6) (dimensionless wellbore pressure response of commingle reservoir):

$$P_{wD}\ t = \frac{Kh}{K_j h_j} \sum_{i=1}^{n} q_{mDi} - q_{mDi-1}\ P_{wcD}\ t_D - t_{Di-1}$$

Substituting equation (3.4.2.1.3) into the above equation yields

$$P_{wD}\ t = \frac{Kh}{K_j h_j} \frac{0.312K_j^{\ 3\ 4}}{\emptyset_j \mu C_t^{\ 1\ 4}\ K_f W_{f\ j}^{\ 1\ 2}} \sum_{i=1}^{n} q_{mDi} - q_{mDi-1}\ t_n - t_{i-1}^{\ 1\ 4} \qquad (3.4.2.1.4)$$

Substituting for dimensionless variables and simplifying further yields

$$\frac{P_i - P_{wf}(t)}{\Delta q_{mj}(t)} = \frac{44.1\mu B}{h_j\ \emptyset_j \mu C_t K_j^{\ 1\ 4}\ K_f W_{f\ j}^{\ 1\ 2}} \sum_{i=1}^{n} \frac{q_i - q_{i-1}}{q_{ref}}\ t_n - t_{i-1}^{\ 1\ 4} \qquad (3.4.2.1.5)$$

Cartesian Analysis

Now, let $m_{Bl} = \frac{44.13\mu B}{h_j\ \emptyset_j \mu C_t K_j^{\ 1\ 4}\ K_f W_{f\ j}^{\ 1\ 2}}$ and $X_{nBl} = \sum_{i=1}^{n} \frac{q_i - q_{i-1}}{q_{ref}}\ t_n - t_{i-1}^{\ 1\ 4}$

Equation (3.4.2.1.5) then becomes

$$J_{wj} = m_{Bl} X_{nBl} \qquad (3.4.2.1.6)$$

Hence, a plot of $J_{wj}(or\ RNP)$ versus $X_{nBl}(RCTF)$ on a cartesian graph yields a straight line of slope m_{Bl} of which the fracture conductivity of layer j can be estimated as

$$K_f W_{f\ j} = \frac{1947.46}{\emptyset_j \mu C_t K_j^{\ 1\ 2}} \left(\frac{\mu B}{h_j m_{Bl}}\right)^2 \quad (3.4.2.1.7)$$

Derivative Analysis

Now, let $t_{eq(Bl)} = e^{X_{nBl}}$; then $\ln t_{eq(Bl)} = X_{nBl}$

Equation (3.4.2.1.6) then becomes

$$J_{wj} = m_{Bl} \ln t_{eq(Bl)} \quad (3.4.2.1.8)$$

Differentiating equation (3.4.2.1.8) with respect to $\ln t_{eq(Bl)}$ yields

$$\frac{dJ_{wj}}{d \ln t_{eq(Bl)}} = J'_{wj} * t_{eq(Bl)} = m_{Bl} \quad (3.4.2.1.9)$$

Equation (3.4.2.1.9) shows that during the bilinear flow, a constant which is a horizontal line on the rate normalized pressure derivative is observed. Equation (3.4.2.1.9) has not been reported in the literature. This equation simplifies the analysis in that it eliminates the need for calculating the slope as is conventionally done.

Now, substituting for m_{Bl} and solving for fracture conductivity yields

$$K_f W_{f\ j} = \frac{1947.46}{\emptyset_j \mu C_t K_j^{\ 1\ 2}} \left(\frac{\mu B}{h_j\ J'_{wj} * t_{eq(Bl)}}\right)^2 \quad (3.4.2.1.10)$$

Log-log Analysis

Now, taking the logarithm of both sides of equation (3.4.2.1.6)yields

$$\log J_{wj} = \log m_{Bl} + \log X_{nBl} \quad (3.4.2.1.11)$$

Hence, a slope of 1 is observed during the bilinear flow regime when J_{wj} is plotted against X_{nBl} on a log-log graph.

At $X_{nBl} = 1$, equation (3.4.2.1.11) becomes

$$J_{wj}{}_{Bl1} = m_{Bl} \quad (3.4.2.1.12)$$

Now substituting and solving for the fracture conductivity

$$K_f W_f{}_j = \frac{1947.46}{\emptyset_j \mu C_t K_j{}^{1}{}_{2}} \left(\frac{\mu B}{h_j J_{wj}{}_{Bl1}}\right)^2 \quad (3.4.2.1.13)$$

Semi-log Analysis

Now, let $t_{eq(Bl)} = 10^{X_{nBl}}$; then $\log t_{eq(Bl)} = X_{nBl}$

Equation (3.4.2.1.6) then becomes

$$J_{wj} = m_{Bl} \log t_{eq(Bl)} \quad (3.4.2.1.14)$$

Hence, a plot of J_{wj} against $t_{eq(Bl)}$ on semilog yields a slope of m_{Bl} of which the fracture conductivity can be solved as

$$K_f W_f{}_j = \frac{1947.46}{\emptyset_j \mu C_t K_j{}^{1}{}_{2}} \left(\frac{\mu B}{h_j m_{Bl}}\right)^2 \quad (3.4.2.1.15)$$

3.4.2.2 Formation Linear flow

To account for the formation linear flow and subsequent estimation of half fracture length, it is reasonable to assume the equation relating the dimensionless wellbore pressure at constant flow rate during the formation linear flow and substitute it into the dimensionless wellbore pressure of commingle reservoir.

Assuming the flow regime in layer j is linear; then we have, as shown by (Gringarten and Ramey[12]

$$P_{wcD} = \overline{\pi t_{Dxf}} \qquad (3.4.2.2.1)$$

Substituting for dimensionless variables on the right hand side only yields

$$P_{wcD} = \frac{0.0288 K_j^{\,1/2}}{\emptyset_j \mu C_t K_j^{\,1/2} X_f} \left(t_n - t_{n-1} \right)^{1/2} \qquad (3.4.2.2.2)$$

Substituting equation 3.4.2.2.2 into equation (3.4.6) yields

$$\frac{P_i - P_{wf}(t)}{\Delta q_{mj}(t)} = \frac{4.064B}{h_j X_{fj}} \left(\frac{\mu}{\emptyset_j C_t K_j} \right)^{1/2} \sum_{i=1}^{n} \frac{q_i - q_{i-1}}{q_{ref}} \left(t_n - t_{i-1} \right)^{1/2} \qquad (3.4.2.2.3)$$

Cartesian Analysis

Let $m_l = \frac{4.064B}{h_j X_f} \left(\frac{\mu}{\emptyset_j C_t K_j} \right)^{1/2}$ and $X_{nl} = \sum_{i=1}^{n} \frac{q_i - q_{i-1}}{q_{ref}} \left(t_n - t_{i-1} \right)^{1/2}$

Equation (3.4.2.2.3) then becomes

$$J_{wj} = m_l X_{nl} \qquad (3.4.2.2.4)$$

Hence, a plot of $J_{wj}(orRNP)$ versus $X_{nl}(RCTF)$ on a cartesian graph yields a straight line of slope m_l of which the half fracture length of layer j can be estimated as

$$X_{fj} = \frac{4.064B}{h_j m_l} \left(\frac{\mu}{\emptyset_j C_t K_j} \right)^{1\ 2} \qquad (3.4.2.2.5)$$

Derivative Analysis

Now, let $t_{eq(l)} = e^{X_{nl}}$; then $\ln t_{eq(l)} = X_{nl}$

Equation (3.4.2.2.4) then becomes

$$J_{wj} = m_l \ln t_{eq(l)} \qquad (3.4.2.2.6)$$

Differentiating equation (3.4.2.2.6) with respect to $\ln t_{eq(l)}$ yields

$$\frac{dJ_{wj}}{d \ln t_{eq(l)}} = J'_{wj} * t_{eq(l)} = m_l \qquad (3.4.2.2.7)$$

Equation (3.4.2.2.7) shows that during the bilinear flow, a constant which is a horizontal line on the rate normalized pressure derivative is observed. This equation simplifies the analysis in that it eliminates the need for calculating the slope as is conventionally done.

Now, substituting for m_l and solving for half fracture length yields

$$X_{fj} = \frac{4.064B}{h_j \ J'_{wj} * t_{eq(l)}} \left(\frac{\mu}{\emptyset_j C_t K_j} \right)^{1\ 2} \qquad (3.4.2.2.8)$$

Log-log Analysis

Now, taking the logarithm of both sides of equation (3.4.2.2.4) yields

$$\log J_{wj} = \log m_l + \log X_{nl} \qquad (3.4.2.2.9)$$

Hence, a slope of 1 is observed during the linear flow regime when J_{wj} is plotted against X_{nl} on a log-log graph.

At $X_{nl} = 1$, equation (3.4.2.2.10) becomes

$$J_{wj}{}_{l1} = m_l \qquad (3.4.2.2.11)$$

Now substituting and solving for the half fracture length

$$X_{fj} = \frac{4.064B}{h_j \; J_{wj}{}_{l1}} \; \frac{\mu}{\emptyset_j C_t K_j}^{1\ 2} \qquad (3.4.2.2.12)$$

Semi-log Analysis

Now, let $t_{eq(l)} = 10^{X_{nl}}$; then $\log t_{eq(l)} = X_{nl}$

Equation 3.4.2.2.6 then becomes

$$J_{wj} = m_l \log t_{eq(l)} \qquad (3.4.2.2.13)$$

Hence, a plot of J_{wj} against $t_{eq(l)}$ on semilog graph yields a slope of m_l of which the fracture conductivity can be solved as

$$X_{fj} = \frac{4.064B}{h_j m_l} \; \frac{\mu}{\emptyset_j C_t K_j}^{1\ 2} \qquad (3.4.2.2.14)$$

3.4.3 Partially Penetrating Fracture

In layered reservoir, some layers may be partially fractured while others may be fully fractured and others may not be fractured at all. For instance, the uppermost and bottom layer may be partially fractured due to gas and water coning respectively. The result is that the individual layers will exhibit varying flow regimes at early times. Assumption of a single model for all the layers is erroneous and will yield inaccurate estimation of the layered properties.

3.4.3.1 Bilinear flow

The dimensionless wellbore pressure during the bilinear flow of a partially penetrating fracture at constant flow rate is given by Rodriguez et al[13]

$$P_{wcD} = \frac{1}{h_{fD}} \frac{2.45}{\overline{C_{fDj}}} t_{Dxf}^{\frac{1}{4}} \qquad (3.4.3.1.1)$$

Where $h_{fD} = \frac{h_{fj}}{hj}$; h_{fj} is the height of fracture in layer j and h_j is the height of layer j.

Substituting for dimensionless variables on the right hand side only yields

$$P_{wcD} = \frac{h_j}{h_{fj}} \frac{0.312 K_j^{\frac{3}{4}}}{K_f W_{f\ j}^{\frac{1}{2}}} t^{\frac{1}{4}} \qquad (3.4.3.1.2)$$

Equation (3.4.3.1.2) can be rewritten in the discretized form as

$$P_{wcD}\ t_{Di} - t_{Di-1} = \frac{h_j}{h_{fj}} \frac{0.312 K_j^{\frac{3}{4}}}{\emptyset_j \mu C_t^{\frac{1}{4}}\ K_f W_{f\ j}^{\frac{1}{2}}} t_n - t_{i-1}^{\frac{1}{4}} \qquad (3.4.3.1.3)$$

Now recalling equation (3.4.6) (dimensionless wellbore pressure of commingle reservoir):

$$P_{wD}\ t\ = \frac{Kh}{K_j h_j} \sum_{i=1}^{n} q_{mDi} - q_{mDi-1}\ \ P_{wcD}\ t_D - t_{Di-1}$$

Substituting equation (3.4.3.1.3) into equation (3.4.6) yields

$$P_{wD}\ t\ = \frac{Kh}{K_j h_j}\ \frac{h_j}{h_{fj}}\ \ \frac{0.312 K_j^{\ 3\ 4}}{\emptyset_j \mu C_t^{\ 1\ 4}\ K_f W_{f\ j}^{\ 1\ 2}} \sum_{i=1}^{n} q_{mDi} - q_{mDi-1}\ \ t_n - t_{i-1}^{\ 1\ 4} \quad (3.4.3.1.4)$$

Substituting for dimensionless variables and simplifying further yields

$$\frac{P_i - P_{wf}(t)}{\Delta q_{mj}(t)} = \frac{44.1 \mu B}{h_{fj}\ \emptyset_j \mu C_t K_j^{\ 1\ 4}\ K_f W_{f\ j}^{\ 1\ 2}} \sum_{i=1}^{n} \frac{q_i - q_{i-1}}{q_{ref}}\ \ t_n - t_{i-1}^{\ 1\ 4} \quad (3.4.3.1.5)$$

Cartesian Analysis

Now, let $m_{Bl} = \frac{44.13 \mu B}{hf_j\ \emptyset_j \mu C_t K_j^{\ 1\ 4}\ K_f W_{f\ j}^{\ 1\ 2}}$ and $X_{nBl} = \sum_{i=1}^{n} \frac{q_i - q_{i-1}}{q_{ref}}\ \ t_n - t_{i-1}^{\ 1\ 4}$

Equation (3.4.3.1.5)then becomes

$$J_{wj} = m_{Bl} X_{nBl} \quad (3.4.3.1.6)$$

Hence, a plot of $J_{wj}(RNP)$ versus $X_{nBl}(RCTF)$ on a cartesian graph yields a straight line of slope m_{Bl} of which the fracture conductivity of layer j can be estimated as

$$K_f W_{f\ j} = \frac{1947.46}{\emptyset_j \mu C_t K_j^{\ 1\ 2}}\ \frac{\mu B}{h_{fj} m_{Bl}}^{\ 2} \quad (3.4.3.1.7)$$

Derivative Analysis

Now, let $t_{eq(Bl)} = e^{X_{nBl}}$; then $\ln t_{eq(Bl)} = X_{nBl}$

Equation (3.4.3.1.6) then becomes

$$J_{wj} = m_{Bl} \ln t_{eq(Bl)} \qquad (3.4.3.1.8)$$

Differentiating equation (3.4.3.1.8) with respect to $\ln t_{eq(Bl)}$ yields

$$\frac{dJ_{wj}}{d \ln t_{eq(Bl)}} = J'_{wj} * t_{eq(Bl)} = m_{Bl} \qquad (3.4.3.1.9)$$

Equation (3.4.3.1.9) shows that during the bilinear flow, a constant which is a horizontal line on the rate normalized pressure derivative is observed. This equation simplifies the analysis in that it eliminates the need for calculating the slope as is conventionally done.

Now, substituting for m_{Bl} and solving for fracture conductivity yields

$$K_f W_{f\ j} = \frac{1947.46}{\emptyset_j \mu C_t K_j^{\ 1\ 2}} \ \frac{\mu B}{h_{fj}\ J'_{wj} * t_{eq(Bl)}}^{\ 2} \qquad (3.4.3.1.10)$$

Log-log Analysis

Now, taking the logarithm of both sides of equation (3.4.3.1.6) yields

$$\log J_{wj} = \log m_{Bl} + \log X_{nBl} \qquad 3.4.3.1.11$$

Hence, a slope of 1 is observed during the bilinear flow regime when J_{wj} is plotted against X_{nBl} on a log-log graph.

At $X_{nBl} = 1$, equation (3.4.3.1.11)becomes

$$J_{wj\ \ Bl1} = m_{Bl} \tag{3.4.3.1.12}$$

Now substituting and solving for the fracture conductivity

$$K_f W_{f\ \ j} = \frac{1947.46}{\left(\emptyset_j \mu C_t K_j\right)^{\frac{1}{2}}} \left(\frac{\mu B}{h_{fj}\ J_{wj\ \ Bl1}}\right)^2 \tag{3.4.3.1.13}$$

Semi-log Analysis

Now, let $t_{eq(Bl)} = 10^{X_{nBl}}$; then $\log t_{eq(Bl)} = X_{nBl}$

Equation (3.4.3.1.6) then becomes

$$J_{wj} = m_{Bl} \log t_{eq(Bl)} \tag{3.4.3.1.14}$$

Hence, a plot of J_{wj} against $t_{eq(Bl)}$ on semilog plot yields a slope of m_{Bl} of which the fracture conductivity can be solved as

$$K_f W_{f\ \ j} = \frac{1947.46}{\left(\emptyset_j \mu C_t K_j\right)^{\frac{1}{2}}} \left(\frac{\mu B}{h_{fj} m_{Bl}}\right)^2 \tag{3.4.3.1.15}$$

3.4.3.2 Formation Linear flow

The dimensionless wellbore pressure during linear flow of a partially penetrating fracture at constant flow rate is given by Raghavan et al[14]

$$P_{wcD} = \frac{h_j}{h_{fj}} \overline{\pi t_{Dxf}} \tag{3.4.3.2.1}$$

Substituting for dimensionless variables on the right hand side only yields

$$P_{wcD} = \frac{h_j}{h_{fj}} \frac{0.0288K_j^{\ 1\ 2}}{\emptyset_j \mu C_t K_j^{\ 1\ 2} X_f} t_n - t_{i-1}^{\ 1\ 2} \quad (3.4.3.2.2)$$

Substituting equation (3.4.3.2.2) into equation (3.4.6) yields

$$\frac{P_i - P_{wf}(t)}{\Delta q_{mj}(t)} = \frac{4.064B}{h_j X_{fj}} \frac{h_j}{h_{fj}} \frac{\mu}{\emptyset_j C_t K_j}^{\ 1\ 2} \sum_{i=1}^{n} \frac{q_i - q_{i-1}}{q_{ref}} t_n - t_{i-1}^{\ 1\ 2} \quad (3.4.3.2.3)$$

Cartesian Analysis

Let $m_l = \frac{4.064B}{h_{fj}X_{fj}} \frac{\mu}{\emptyset_j C_t K_j}^{\ 1\ 2}$ and $X_{nl} = \sum_{i=1}^{n} \frac{q_i - q_{i-1}}{q_{ref}} t_n - t_{i-1}^{\ 1\ 2}$

Equation 3.4.3.2.3 then becomes

$$J_{wj} = m_l X_{nl} \quad (3.4.3.2.4)$$

Hence, a plot of $J_{wj}(RNP)$ versus $X_{nl}(RCTF)$ on a cartesian graph yields a straight line of slope m_l of which the half fracture length of layer j can be estimated as

$$X_{fj} = \frac{4.064B}{h_{fj} m_l} \frac{\mu}{\emptyset_j C_t K_j}^{\ 1\ 2} \quad (3.4.3.2.5)$$

Derivative Analysis

Now, let $t_{eq(l)} = e^{X_{nl}}$; then $\ln t_{eq(l)} = X_{nl}$

Equation(3.4.3.2.4) then becomes

$$J_{wj} = m_l \ln t_{eq(l)} \quad (3.4.3.2.6)$$

Differentiating equation (3.4.3.2.6) with respect to $\ln t_{eq(l)}$ yields

$$\frac{dJ_{wj}}{d\ln t_{eq(l)}} = J'_{wj} * t_{eq(l)} = m_l \qquad (3.4.3.2.7)$$

Equation (3.4.3.2.6) shows that during the bilinear flow, a constant which is a horizontal line on the rate normalized pressure derivative is observed. This equation simplifies the analysis in that it eliminates the need for calculating the slope as is conventionally done.

Now, substituting for m_l and solving for half fracture length yields

$$X_{fj} = \frac{4.064B}{h_{fj}\ J'_{wj} * t_{eq(l)}} \left(\frac{\mu}{\emptyset_j C_t K_j}\right)^{1\ 2} \qquad (3.4.3.2.8)$$

Log-log Analysis

Now, taking the logarithm of both sides of equation (3.4.3.2.4) yields

$$\log J_{wj} = \log m_l + \log X_{nl} \qquad (3.4.3.2.9)$$

Hence, a slope of 1 is observed during the linear flow regime when J_{wj} is plotted against X_{nl} on a log-log graph.

At $X_{nl} = 1$, equation (3.4.3.2.9) becomes

$$J_{wj\ \ l1} = m_l \qquad (3.4.3.2.10)$$

Now substituting and solving for the half fracture conductivity

$$X_{fj} = \frac{4.064B}{h_{fj}\ J_{wj\ \ L1}} \left(\frac{\mu}{\emptyset_j C_t K_j}\right)^{1\ 2} \qquad (3.4.3.2.11)$$

Semi-log Analysis

Now, let $t_{eq(l)} = 10^{X_{nl}}$; then $\log t_{eq(l)} = X_{nl}$

Equation (3.4.3.2.4) then becomes

$$J_{wj} = m_{Bl} \log t_{eq(l)} \qquad (3.4.3.2.11)$$

Hence, a plot of J_{wj} against $t_{eq(l)}$ on semilog graph yields a slope of m_l of which the fracture conductivity can be solved as

$$X_{fj} = \frac{4.064B}{h_{fj} m_l} \left(\frac{\mu}{\emptyset_j C_t K_j} \right)^{1\ 2} \qquad (3.4.3.2.11)$$

3.5 Layer Wellbore Storage

The measured flow rate is related to the sandface flow rate for a constant wellbore storage effect as (Kuchuk et al[17]):

$$q_{sf} - q_m = C \frac{dP_{wf}}{dt} \qquad (3.4.1.21)$$

Rearranging equation (3.4.1.21) yields

$$q_m = q_{sf} - C \frac{dP_{wf}}{dt} \qquad (3.4.1.22)$$

Hence a plot of qm versus the derivative of the wellbore pressure yields a straight line of slope a slope, C, which is the wellbore storage co-efficient. The wellbore storage co-efficient computed is due to the fluid volume below the flowmeter.

qm is the measured flow rate above the layer of interest and qsf is the sandface flow rate which is regarded as the flowrate at the reservoir/wellbore interface in this thesis.

The above is used to estimate the wellbore storage co-efficient of the fluid volume below the flowmeter and not the entire wellbore volume.

3.6 Deconvolution

Unlike the convolution technique, the deconvolution technique does not assume a model; instead, it calculates the influence function, $\Delta P'_{sf}$, which is used in the standard methodologies to diagnose the model and calculate the unknown reservoir and well parameters. For instance, in a fractured multilayered reservoir, the logarithmic convolution cannot model the bilinear and linear flow geometries but with the use of the deconvolution technique, the influence function (constant-rate solution) is determined which is use to diagnose the appropriate model for the estimation of the individual layer properties. Deconvolution also minimizes wellbore storage effect.

Both the discretized form and Laplace domain will be used to determine the influence function.

3.6.1 Discretized form

For n intervals of time steps, the discretized form of equation (3.4.5) is given by

$$\Delta P_w\ t\ = \frac{Kh}{K_j h_j}\sum_{i=1}^{n} q_{mD\ n-i+1} - q_{mD\ n-i}\quad F(t_n - t_{n-i}) \qquad (3.6.1.1)$$

But $F\ t_n - t_{n-i}\ = F_i$

F_i is the influence function at the previous time step.

Also, $q_{mD(0)} = 0$, $F_{(0)} = 0$

Now, for the very last time step, $(i = n)$, then equation (3.6.1.1) becomes

$$\Delta P_{w\ n} = \frac{Kh}{K_j h_j} q_{mD1} F_n \tag{3.6.1.2}$$

Hence, equation (3.6.1.1)can be rewritten as

$$\Delta P_{w\ n} = \frac{Kh}{K_j h_j} \sum_{i=1}^{n-1} q_{mD\ n-i+1} - q_{mD\ n-i}\ F_i + q_{mD1} F_n \tag{3.6.1.3}$$

Making F_n (influence function) the subject yields

$$F_n = \frac{\frac{Kh}{K_j h_j}\ \Delta P_{w\ n} - \sum_{i=1}^{n-1} q_{mD\ n-i+1} - q_{mD\ n-i}\ F_i}{q_{mD1}} \tag{3.6.1.4}$$

Hence, the influence function (or constant-rate solution) can be obtained if the pressure drawdown, $\Delta P_{w\ n} = P_i - P_{wfn}$, the measured flow rate, $q_{mD,}$ the average and layer flow capacities and the previous influence function, F_i, are known.

For the first time step, $n = 1$,

$$F_1 = \frac{Kh}{K_j h_j} \frac{\Delta P_{w\ 1}}{q_{mD1}} \tag{3.6.1.5}$$

For the second time step, n=2

$$F_2 = \frac{\frac{Kh}{K_j h_j}\ \Delta P_{w\ 2} - q_{mD2} + q_{mD1}\ F_1}{q_{mD1}} \tag{3.6.1.6}$$

$\ldots\ldots etc$

Having calculated the influence function, the appropriate model can be diagnosed by plotting $F_n$versus time on a log-log plot which can then be used to estimate the layered properties.

Kuchuk et al[17]has suggested the following:

- If the wellbore storage and skin are zero, then

  $F_n = \lambda \ \bar{t}$ is the early time approximation for the solution that is internally bounded by a smooth (fracture) with a constant flow rate boundary.

- If the wellbore storage is zero with a non-zero skin, then

  $F_n = \lambda \ \bar{t} + \Delta P_s$

- If both the wellbore storage and skin are non-zero, then

  $F_n = \alpha t$ is the early-time approximation of the finite wellbore solution with the wellbore storage skin effects. It also approximates the case where the wellbore storage is finite with a zero skin.

- An appropriate general approximation at early times is thus

  $F_n = \alpha t + \lambda \ \bar{t} + \Delta P_s$

$\alpha, and\ \lambda\ are\ constants. \Delta P_s$ is the pressure drop due to skin and F_n is the influence function or constant rate solution or the wellbore pressure drop had the down hole flow rate been constant.

3.6.2 Expressing F_n in the Laplace Domain

The Laplace Transform of equation (3.4.5) is given by

$$\Delta P_w \ s \ = \frac{Kh}{K_j h_j} \ q_{sfD} \ s \ s\Delta P_{sf} \ s \qquad (3.6.2.1)$$

Now, dividing both sides of equation (3.4.1.22) by the reference rate (total rate of all the layers) yields Kuchuk et al[17],

$$q_{sfD} = q_{mD} + \frac{C}{q_{ref}} \frac{dP_w}{dt} \tag{3.6.2.2}$$

Now, taking the Laplace of equation (3.6.2.2) yields Kuchuk et al[17]:

$$q_{sfD}\ s\ = q_{mD}\ s\ + \frac{C}{q_{ref}}\ s\Delta P_w\ s \tag{3.6.2.3}$$

Substituting equation (3.6.2.3) into (3.6.2.1) yields

$$\Delta P_w\ s\ = \frac{Kh}{K_j h_j}\ q_{mD}\ s\ + \frac{C}{q_{ref}}\ s\Delta P_w\ s\ \ s\Delta P_{sf}\ s \tag{3.6.2.4}$$

Hence,

$$\Delta P_{sf}\ s\ = \frac{\Delta P_w\ s}{\frac{Kh}{K_j h_j}\ sq_{mD}\ s\ + \frac{C}{q_{ref}}\ s^2\Delta P_w\ s} \tag{3.6.2.5}$$

In the absence of wellbore storage, the influence function in Laplace space can be found from equation (3.6.2.1) as

$$\Delta P_{sf}\ s\ = \frac{\Delta P_w\ s}{\frac{Kh}{K_j h_j}\ sq_{mD}\ s} \tag{3.6.2.6}$$

$\Delta P_{sf}\ s$ is the influence function in the Laplace space; hence

Stehfest Algorithm can be used to invert the above equation to real time domain and plot against time on a log-log plot to diagnose the model and determine the individual layer properties.

Now, since equation (3.6.2.3) is applicable for constant wellbore storage, equation (3.6.2.5) can only be used if the wellbore storage is constant.

CHAPTER 4 APPLICATION OF THE MATHEMATICAL MODEL: LAYERED PARAMETER ESTIMATION

Example1. The following field data was taken from Ehlig-Economides and Joseph[15], and was conducted on a 5 layered- reservoir.

Table 4.1: Pressure data for layered reservoir for example 1

t,days	Pwf
0.000015	4466.2
0.000063	4458.8
0.000127	4455.2
0.000511	4448.4
0.00205	4441.7
0.0164	4432
0.0328	4428.8
0.131	4422.1
0.524	4410.7
2.097	4371.7
4.194	4321

Fluid viscosity = 1.0 cp

FVF = 1.2 RB/STB

Total compressibility = 2.1*10^-5 /psi

Total flow rate = 500 STB

Solution:

Table 4.2: Pressure and Pressure derivative data for layered reservoir for example 1

t,days	Pwf	ΔP	t*ΔP'
0.00036	4466.2	31.9	
0.001512	4458.8	39.3	5.142
0.003048	4455.2	42.9	5.051
0.012264	4448.4	49.7	4.854
0.0492	4441.7	56.4	4.760
0.03936	4432	66.1	4.629
0.7872	4428.8	69.3	4.691
3.144	4422.1	76	6.530
12.576	4410.7	87.4	18.171
50.328	4371.7	126.4	58.141
100.656	4321	177.1	

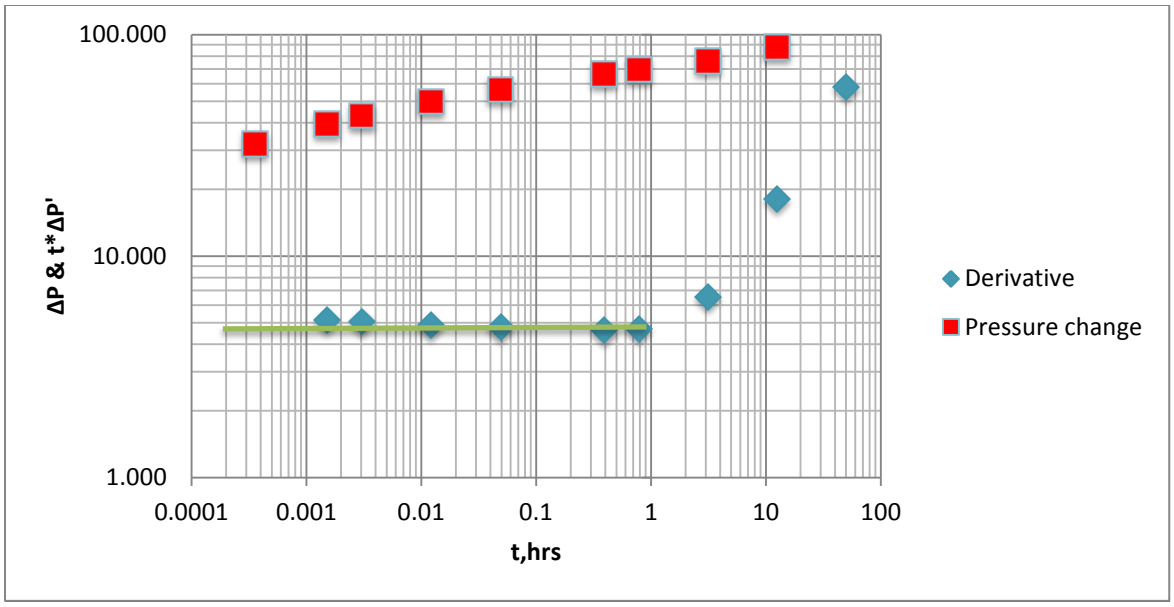

Figure 4.1: log-log plot of pressure and pressure derivative for a drawdown test in a 5-layered reservoir for example 1.

From figure 4.1,

$$\Delta P' * t_{\ r} = 4.8\ psi$$

Hence from equation (3.2.4.16), the average permeability thickness is estimated as

$$Kh = \frac{70.6q\mu B}{\Delta P' * t_{\ r}} = \frac{70.6 * 500 * 1.2 * 1}{4.8}$$

$$= 8{,}825\ \text{md} - \text{ft}$$

Table 4.3: Result of the pressure analysis in a 5-layered reservoir for example 1

	True value	This Study (TDS)	Error (%)	Source (Type Curve)	Error (%)
Kh	10,000	8,825	11.75	8,472	15.28

The above results show that when pressure data alone is used to analyze a multi-layered reservoir, it gives erroneous results regardless of how accurate the technique (TDS or type curves) used.

Example 2

The following field data was taken from Britt and Bennett[5] and was conducted on commingled multi-layered reservoir.

Table 4.4: Rock and fluid properties for example 2

qi	1000	BWIPD
B	1	RB.STB
U	0.75	cp
Ct	0.0000095	/psi
poro	0.09	
k	2.33	md
h	206	ft
RcD	0.89	

TIME (HRS)	PRESSURE (PSIA)
0	1245
0.5	1127
1	1111
2	1085
3	1068
4	1052
5	1038
6	1037
7	1025
8	1017
9	1008
16	976
25	968
36	921
49	903
64	880
70	876

Solution:

Table 4.6: Pressure and Pressure derivative data for layered reservoir for example 2

Time(hrs)	Pressure(psia)	ΔP	t*ΔP'
0	1245	0	
0.5	1127	118	
1	1111	134	16.426
2	1085	160	37.608
3	1068	177	52.196
4	1052	193	52.489
5	1038	207	49.913
6	1037	208	51.885
7	1025	220	58.843
8	1017	228	63.15
9	1008	237	58.669
16	976	269	71.23
25	968	277	78.913
36	921	324	79.505
49	903	342	81.42
64	880	365	
70	876	369	

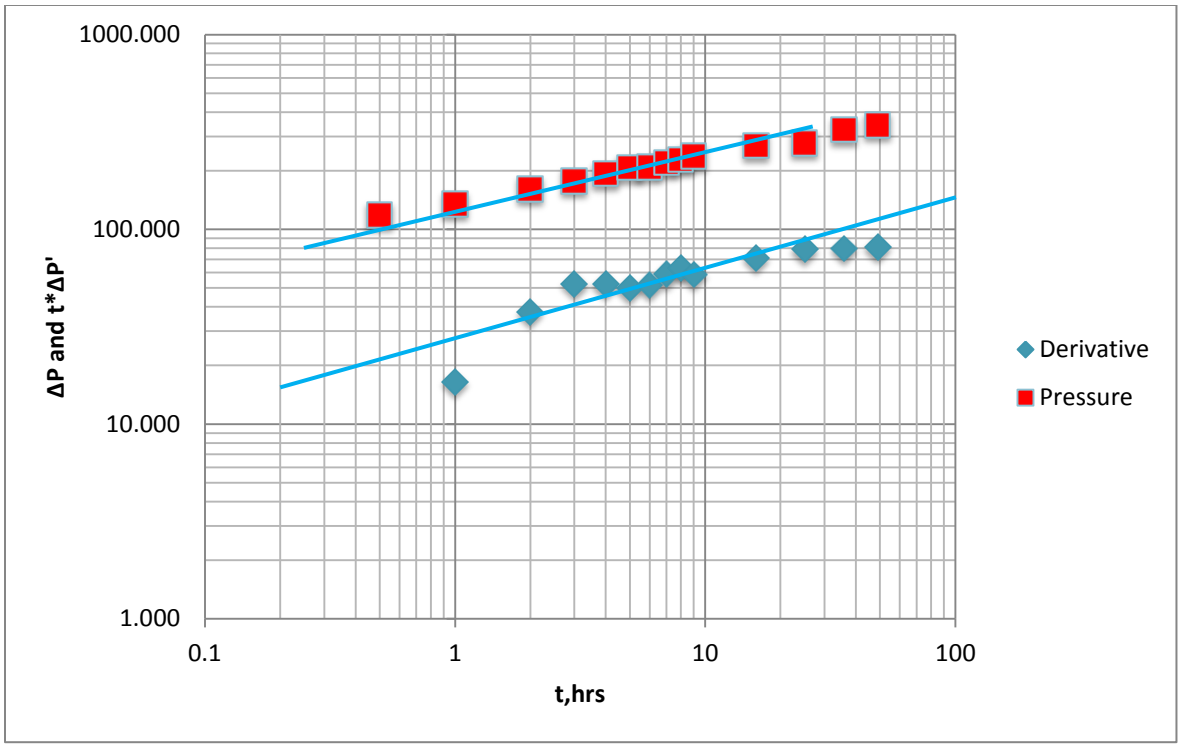

Figure 4.2: log-log plot of pressure and pressure derivative for a drawdown test in a commingle reservoir for example 2.

From figure 4.2, a slope of 0.25 is observed on both the pressure and pressure derivative curve depicting a bilinear flow regime and at t=1hour, the following is read.

$\Delta P_{BL1} = 134\ psia,\ \ t * \Delta P'_{BL1} = 32\ psia$. The fracture conductivity is estimated as follows:

$$K_f W_f = \frac{1947.46}{R_{CD}\sqrt{\emptyset \mu C_t K}} \left(\frac{q\mu B}{h\ \Delta P_{BL1}}\right)^2$$

$$K_f W_f = \frac{1947.46}{0.89 * (\sqrt{0.09 * 0.75 * 0.0000085 * 2.33})} \left(\frac{1000 * 0.75 * 1}{206 * 134}\right)^2$$

$$K_f W_f = 1321\ md - ft$$

This value is only an average of the total system

Example 3:

The following synthetic data was taken from Okoye et al[19] and was conducted on a single layered reservoir.

Table 4.7: Rock and fluid properties for example 3

$r_w = 0.032\ ft$

q	250	STB/D
B	1.65	RB/STB
μ	0.85	cp
Ct	0.00002	/psi
Ø	0.3	
h	30	ft

Table 4.8: Pressure data for layered reservoir for example 3

Time (HRS)	Pi-**Pwf** **(Psi)**
0.25	57
0.5	68
1	79
2.5	106
5	134

10	168
20	210
30	238
40	261
50	280
60	298
70	311
80	321
90	334
100	343
150	384

Solution

Table 4.9: Pressure and Pressure derivative data for layered reservoir for example 3

Time (HRS)	Pi-**Pwf** **(Psi)**	ΔP'	t*ΔP'
0.25	57		
0.5	68	36.66667	18.33333
1	79	21	21
2.5	106	15.45	38.625
5	134	9.733333	48.66667
10	168	5.933333	59.33333
20	210	3.5	70

30	238	2.55	76.5
40	261	2.1	84
50	280	1.85	92.5
60	298	1.55	93
70	311	1.15	80.5
80	321	1.15	92
90	334	1.1	99
100	343	0.886667	88.66667
150	384		

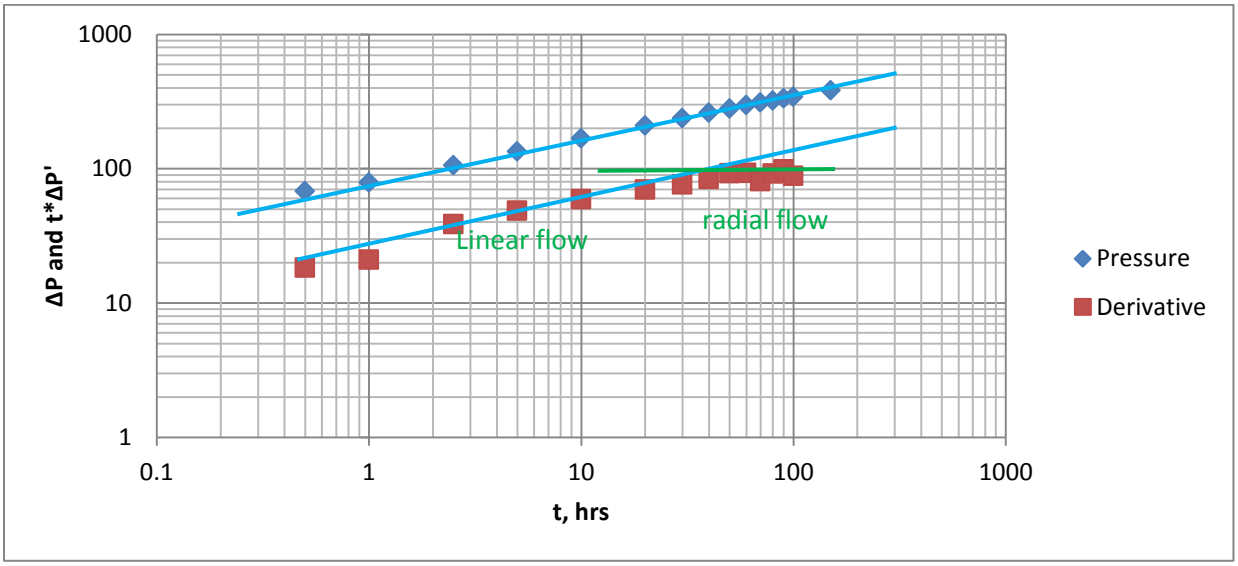

Figure 4.3: log-log plot of pressure and pressure derivative for a drawdown test in a single-layered reservoir for example 3.

The above plot is similar to the plots preceding it; the point worthy of note is that unless the duration of flow is long enough (as is depicted in figure 1), a single layered reservoir has similar pressure signature to multi-layered reservoir.

Example 4

The following table is a production profile of a 3-layered commingled reservoir.

Table 4.10: Pressure and layered flowrate data for layered reservoir for example 4

t,days	t,hrs	Pwf	ΔP	Layer1 q1(B/D)	Layer2 q2(B/D)	Layer3 q3(B/D)		
0.00	0	4498.1	0.00	0.00	0.00	0.00		
0.000015	0.00036	4466.2	31.9	158.3	92.85	104.4		
0.000063	0.001512	4458.8	39.3	150.6	104.9	101.9		
0.000127	0.003048	4455.2	42.9	147.6	109.9	100.7		
0.000511	0.012264	4448.4	49.7	142.5	118.3	98.68		
0.00205	0.0492	4441.7	56.4	138.4	125.3	96.88		
0.0164	0.3936	4432	66.1	133.5	133.9	94.69		
0.0328	0.7872	4428.8	69.3	132.1	136.4	94.14		
0.131	3.144	4422.1	76	129.67	139.7	93.69		
0.524	12.576	4410.7	87.4	125.93	137.3	94.75		
2.097	50.328	4371.7	126.4	115.04	125.2	101.8		
4.194	100.656	4321	177.1	107.33	117.1	107.8		

Table 4.11: Rock properties for example 4

Layer	Ø	Height (ft)
1	0.3	10
2	0.1	10
3	0.1	10
4	0.25	10
5	0.25	10

Fluid Properties: μ =1.0 cp; Ct =2.1*10^-5 /psi: FVF = 1.2 rb/STB; rw = 0.333ft

Solution:

Both the logarithmic convolution and Tiab's Direct Synthesis will be used to analyze the problem.

Layer 1Analysis

Table 4.12: Layer 1Rate normalized pressure and rate normalized pressure derivative data for example 4

t,hrs	teq,hrs	RCTF	Jw1	(teq*Jw1)'
0.00036	0.081232	-1.09027	0.201516	
0.001512	0.142004	-0.8477	0.260956	
0.003048	0.181931	-0.74009	0.29065	0.125
0.012264	0.286463	-0.54293	0.348772	0.134
0.0492	0.435884	-0.36063	0.407514	0.146
0.3936	0.780929	-0.10739	0.495131	0.152
0.7872	0.941335	-0.02626	0.524603	0.167
3.144	1.348576	0.129875	0.586103	0.241
12.576	1.896977	0.278062	0.694036	0.842
100.656	2.728733	0.435961	1.650051	

Cartesian Approach:

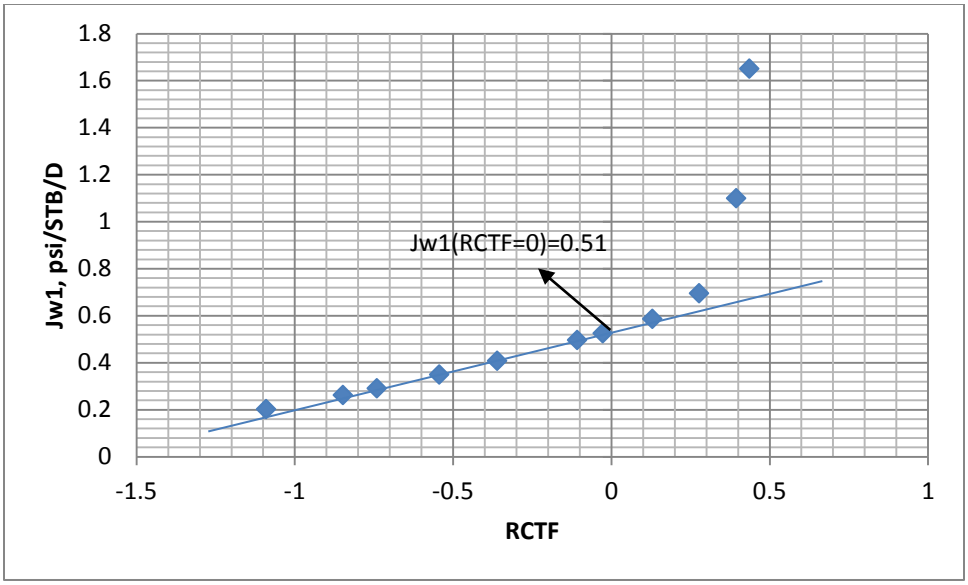

Figure 4.4: A Cartesian plot of RNP Versus RCTF for example 4

From figure 4.4, the slope is calculated as follows:

$$m = \frac{0.201516 - 0.524603}{-1.09027 - (-0.02626)} = 0.30365\ psi/STB/D/RTCF$$

Hence the permeability of layer 1 is estimated as:

$$K_1 = \frac{162.6 * 1 * 1.2}{10 * 0.30365} = 64\ mD$$

The layer 1 skin is also calculated as follows:

From figure 1, $J_{w1}\ \ RCTF = 0\ \ = 0.51\ psi/STB/D$

Hence, the layer 1 skin is estimated using equation (3.4.1.9) as:

$$S_1 = 1.1513\ \frac{0.51}{0.30365} - \log\ \frac{64}{0.3 * 1 * 1.2 * 10^{-5} * 0.333\text{^}2}\ + 3.2275$$

$$= -3.8$$

Semilog Approach:

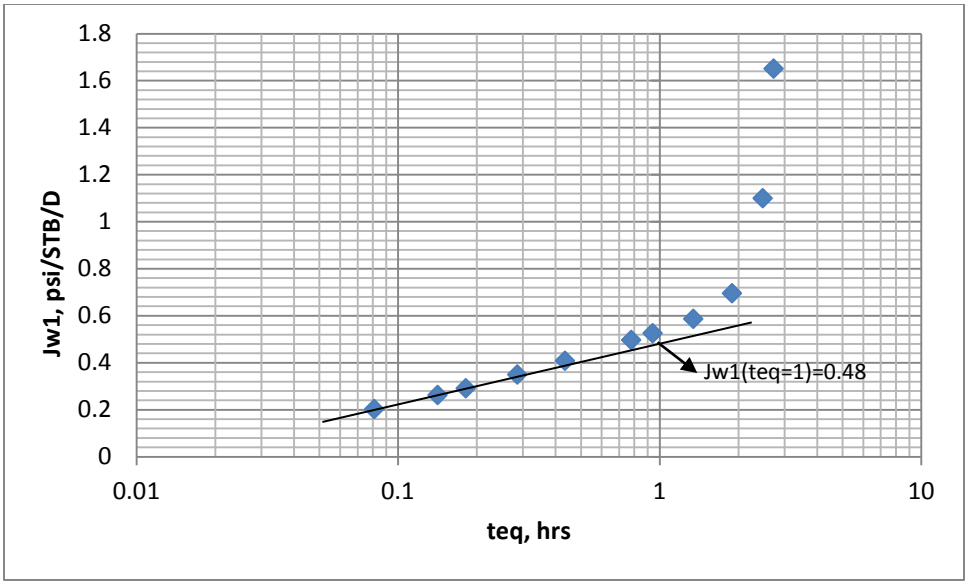

Figure 4.5: A Semilog plot of RNP Versus teq

The slope of figure is estimated as

$$m = \frac{0.48 - 0.201516}{1 - 0.081232} = 0.303106\ psi/STB/D/RTCF$$

Hence the permeability of layer 2 is estimated as:

$$K_1 = \frac{162.6 * 1 * 1.2}{10 * 0.303106} = 64.4\ mD$$

The layer skin is then estimated using equation (3.4.1.12) as:

From figure 4.5, $J_{w1}\ \ t_{eq} = 1\ \ = 0.48\ psi/STB/D$

$$S_1 = 1.1513\ \ \frac{0.48}{0.303106} - \log\ \ \frac{64}{0.3 * 1 * 1.2 * 10^{-5} * 0.333\text{^}2}\ \ + 3.2275$$

$$S_1 = -3.9$$

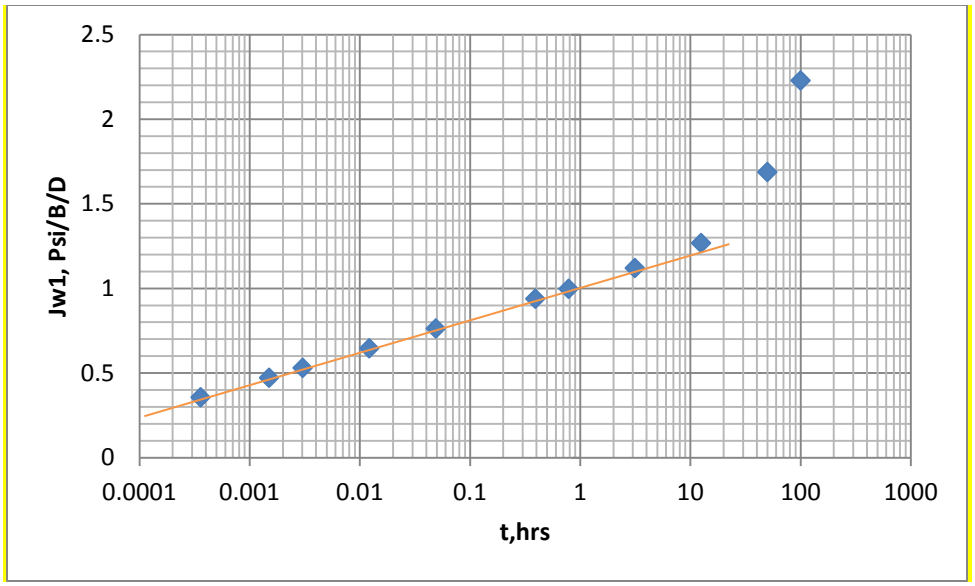

Figure 4.6: A Cartesian plot of RNP Versus t

Figure 4.6 depicts that instead of the equivalent time function, teq, the actual time can be used for the analysis. However, if the equivalent time function, teq, is available, it is recommended to use it.

Tiab's Direct Synthesis Technique:

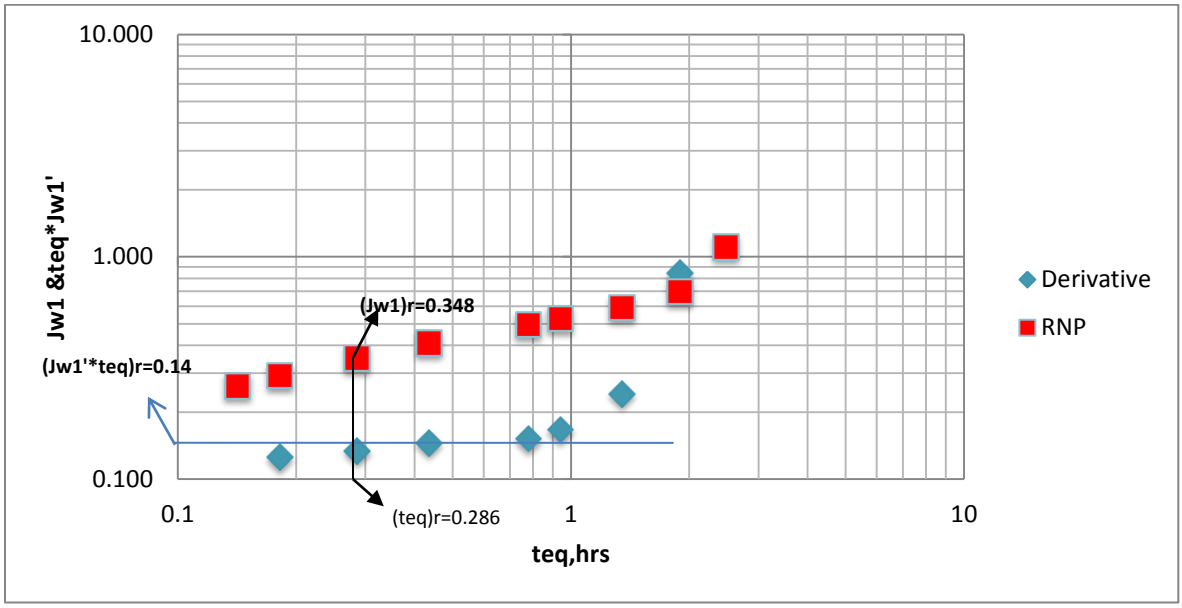

Figure 4.7: A log-log plot for RNP and RNP derivative against teq

From figure 4.7,

$$J'_{w1} * t_{eq\ \ r} = 0.14$$

The permeability of layer 1 can now be estimated from equation (3.4.1.16) as:

$$K_1 = \frac{70.6 * 1.0 * 1.2}{10 * 0.14} = 60.5\ mD$$

The skin layer 1 can also be estimated from equation (3.4.1.21) as:

$$s_1 = 0.5\ \frac{0.348}{0.14} - \ln\ \frac{60.5 * 0.286}{0.3 * 1 * 1.2 * 10^{-5} * 0.333\text{^}2}\ + 7.43$$

$$= -3.8$$

The solution is summarized in the following table and shows that the Tiab's Direct Synthesis has successfully been applied to the problem and is having a good match with the logarithmic convolution solution.

Table 4.13: Layer 1results for rate normalized pressure using different approaches

Parameter	Cartesian Approach	Semilog Approach	TDS
k1 (mD)	64	64.4	60.5
Si	-3.8	-3.9	-3.8

Layer 2 Analysis:

Table 4.14: Rate normalized pressure and rate normalized pressure derivative data for example 4

t,hrs	teq	RTCF	Jw2	teq*Jw2'
0.00036	0.229354	-0.63949	0.343565	
0.001512	0.254345	-0.59458	0.374643	0.12
0.003048	0.277137	-0.55731	0.390355	0.096
0.012264	0.350592	-0.4552	0.420118	0.09
0.0492	0.467503	-0.33022	0.45012	0.098
0.3936	0.776753	-0.10972	0.493652	0.098
0.7872	0.93224	-0.03047	0.508065	0.097
3.144	1.181991	0.072614	0.544023	0.095
12.576	1.591287	0.201749	0.636562	0.234
50.328	2.686691	0.429218	1.009585	1.052
100.656	2.987961	0.475375	1.512383	

Cartesian Approach:

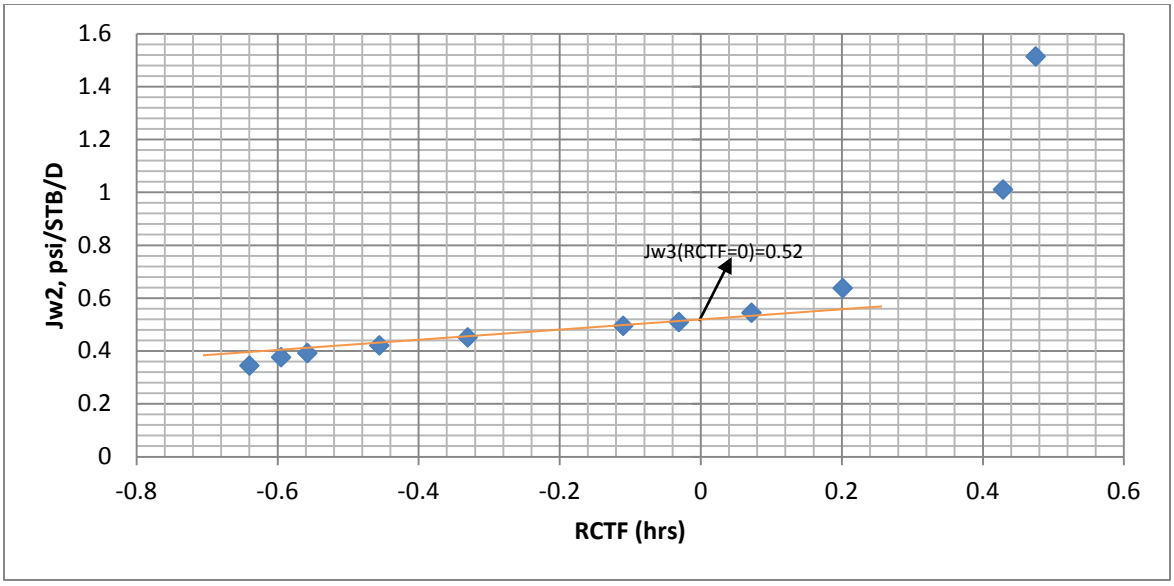

Figure 4.8: A Cartesian plot for RNP against RCTF

From figure 4.8, the slope is calculated as follows:

$$m = \frac{0.544023 - 0.45012}{0.072614 - (-0.33022)} = 0.233\ psi/STB/D/RTCF$$

Hence the permeability of layer 2 is estimated as:

$$K_2 = \frac{162.6 * 1.0 * 1.2}{10 * 0.233} = 83.7\ mD$$

The layer 2 skin is also calculated from equation (3.4.1.9) as follows:

From figure 4.8, $J_{w1}\ \ RCTF = 0\ \ = 0.52\ psi/STB/D$

Hence,

$$S_2 = 1.1513\ \frac{0.52}{0.233} - \log\ \frac{83.7}{0.3 * 1.0 * 1.2 * 10^{-5} * 0.333\text{^}2}\ + 3.2275$$

$$= -3.3$$

Semilog Approach:

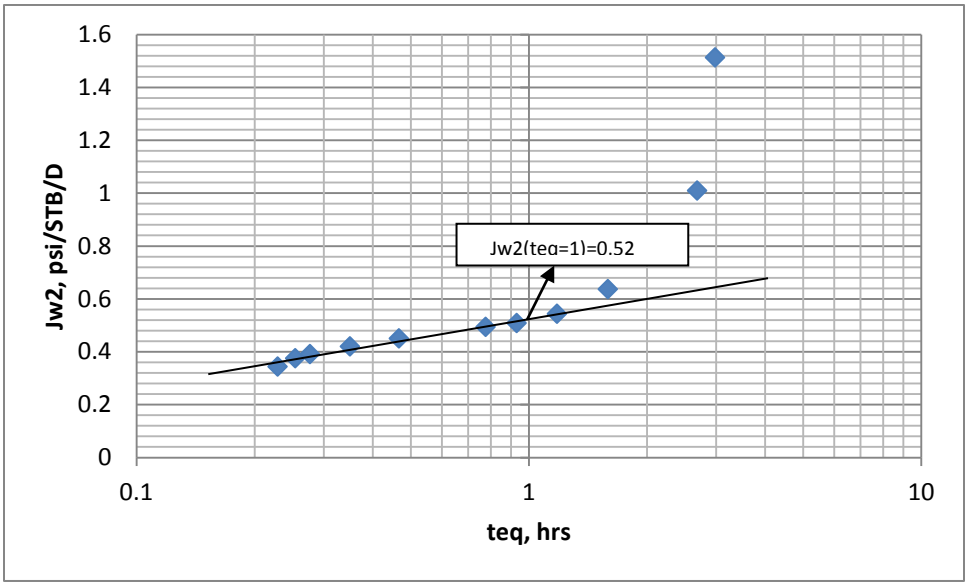

Figure 4.9: A semi-log plot of RNP against teq.

The slope of figure 4.9 is estimated as

$$m = \frac{0.442 - 0.390355}{0.5 - 0.277137} = 0.232\ psi/STB/D/RTCF$$

Hence the permeability of layer 2 is estimated as:

$$K_2 = \frac{162.6 * 1 * 1.2}{10 * 0.232} = 84.1\ mD$$

The layer skin is then estimated

From figure 4.9, $J_{w2}\ \ t_{eq} = 1\ \ = 0.52\ psi/STB/D$

$$S_2 = 1.1513\ \frac{0.52}{0.232} - \log\ \frac{84.1}{0.3 * 1 * 1.2 * 10^{-5} * 0.333\text{^}2}\ + 3.2275$$

$$S_2 = -3.3$$

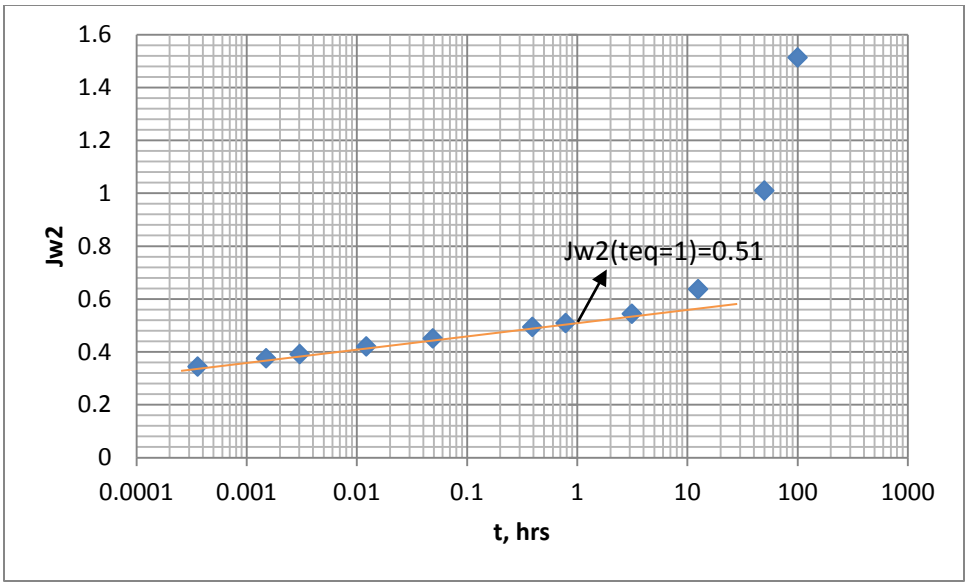

Figure 4.10: A semi-log plot RNP against t

Figure 4.10 depicts that instead of the equivalent time function, teq, the actual time can be used for the analysis. However, if the equivalent time function, teq, is available, it is recommended to use it.

Tiab's Direct Synthesis Technique:

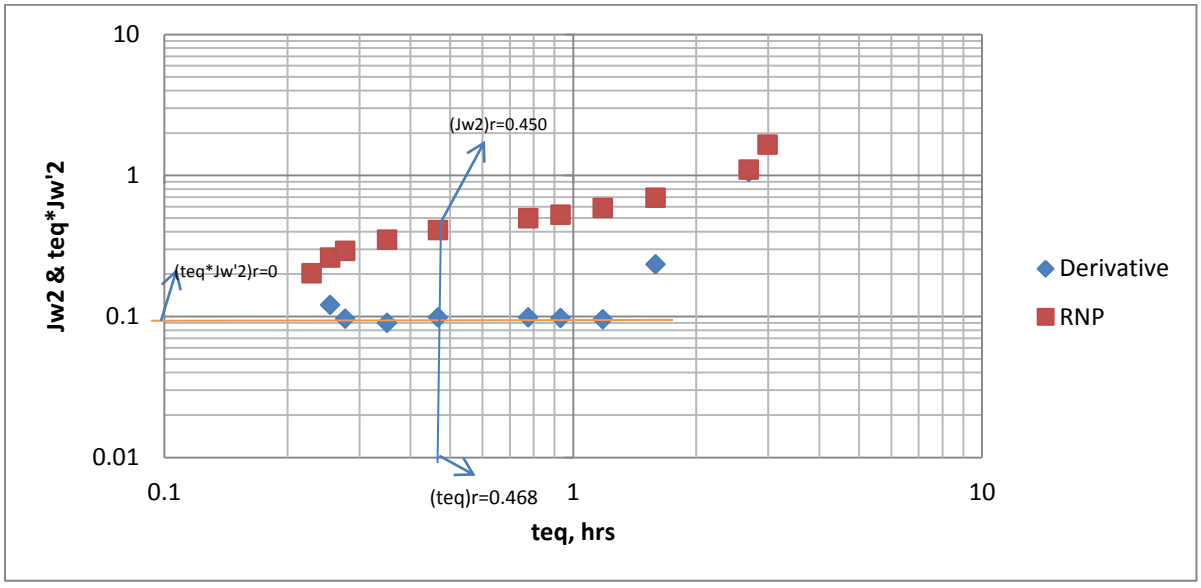

Figure 4.11: A plot of RNP and derivative against teq

From figure 14, $(t_{eq} * J'_{w2})_r = 0.098$

The permeability of layer 2 can now be estimated as:

$$K_2 = \frac{70.6 * 1.0 * 1.2}{10 * 0.098} = 86\ mD$$

The skin layer 2 can also be estimated as:

$$s_2 = 0.5\ \frac{0.450}{0.098} - \ln\ \frac{86 * 0.468}{0.3 * 1 * 1.2 * 10^{-5} * 0.333\text{^}2}\ + 7.43$$

$$= -3.2$$

The solution is summarized in the following table and shows that the Tiab's Direct Synthesis has successfully been applied to the problem and is having a good match with the logarithmic convolution solution.

Table 4.15: Layer 2 results for rate normalized pressure using different approaches

Parameter	Cartesian Approach	Semilog Approach	TDS
K2 (mD)	83.7	84.1	86.0
S2	-3.3	-3.3	-3.2

Layer 3 Analysis:

Table 4.16: Rate normalized pressure and rate normalized pressure derivative data for example 4

t,hrs	teq	RTCF	Jw3	t*Jw'
0.00036	0.190966	-0.71904	0.305556	
0.001512	0.266553	-0.57422	0.385672	0.244
0.003048	0.312081	-0.50573	0.426018	0.259
0.012264	0.420219	-0.37652	0.503648	0.268
0.0492	0.558681	-0.25284	0.582164	0.281
0.3936	0.838754	-0.07637	0.698067	0.286
0.7872	0.957025	-0.01908	0.736138	0.289
3.144	1.240033	0.093433	0.811186	0.356
12.576	1.614911	0.208148	0.922427	0.745
50.328	2.211468	0.344681	1.24165	
100.656	2.67522	0.42736	1.642857	

Now for layer 3, the rate normalized pressure (RNP) can be plotted against the RCTF on Cartesian plot, the equivalent time, teq, and real time on semi log plot as shown below.

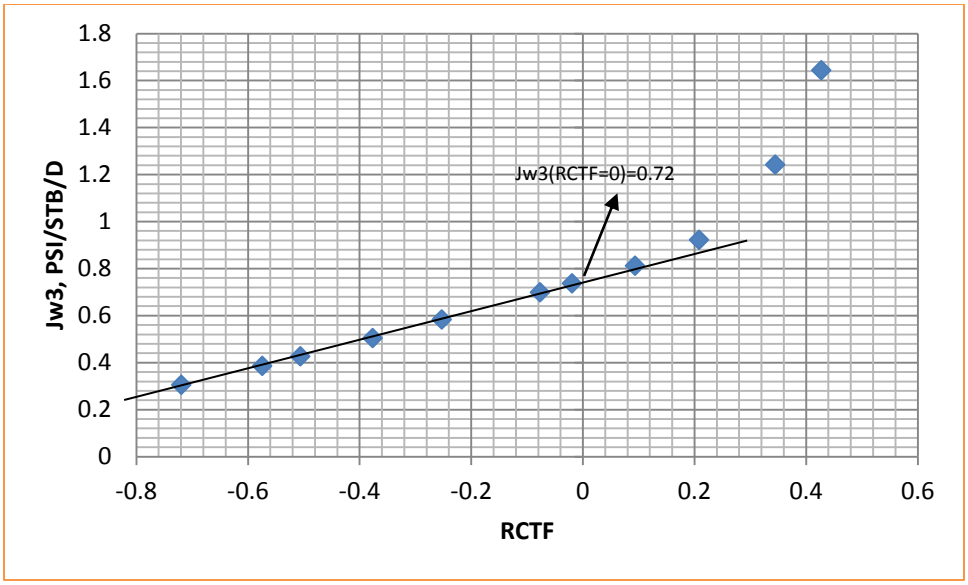

Figure 4.12: A Cartesian plot of RNP against RCTF

From figure 4.12, the slope is calculated as follows:

$$m = \frac{0.736138 - 0.385672}{-0.019077 - (-0.57422)} = 0.631\ psi/STB/D/RTCF$$

Hence the permeability of layer 3 is estimated as:

$$K_3 = \frac{162.6 * 1.0 * 1.2}{10 * 0.631} = 30.9\ mD$$

The layer 3 skin is also calculated as follows:

From figure 4.12, $J_{w1}\ \ RCTF = 0\ \ = 0.72\ psi/STB/D$

Hence,

$$S_3 = 1.1513\ \frac{0.72}{0.631} - \log\ \frac{30.9}{0.3 * 1.0 * 1.2 * 10^{-5} * 0.333\text{^}2}\ + 3.2275$$

$$= -4.0$$

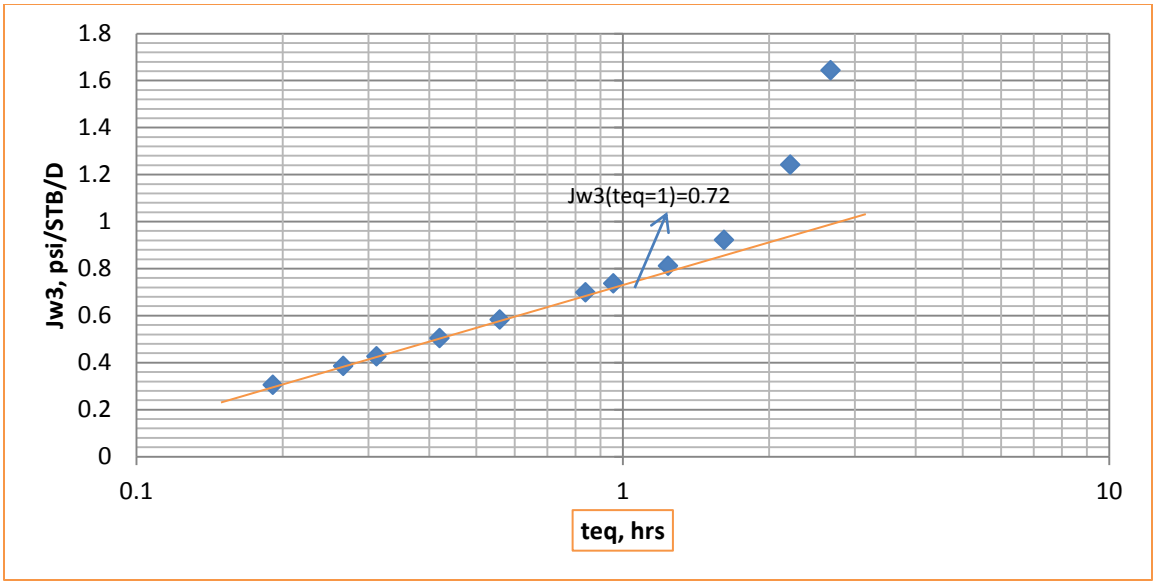

Figure 4.13: A semi-log plot of RNP against teq

The slope of figure 4.13 is estimated as

$$m = \frac{0.59 - 0.385672}{0.6 - 0.266553} = 0.613\ psi/STB/D/RTCF$$

Hence the permeability of layer 3 is estimated as:

$$K_3 = \frac{162.6 * 1 * 1.2}{10 * 0.613} = 31.8\ mD$$

The layer skin is then estimated

From figure 4.13, $J_{w2}\ \ t_{eq} = 1\ \ = 0.72\ psi/STB/D$

$$S_3 = 1.1513\ \frac{0.72}{0.613} - \log\ \frac{31.8}{0.3 * 1 * 1.2 * 10^{-5} * 0.333\text{^}2}\ + 3.2275$$

$$S_3 = -4.0$$

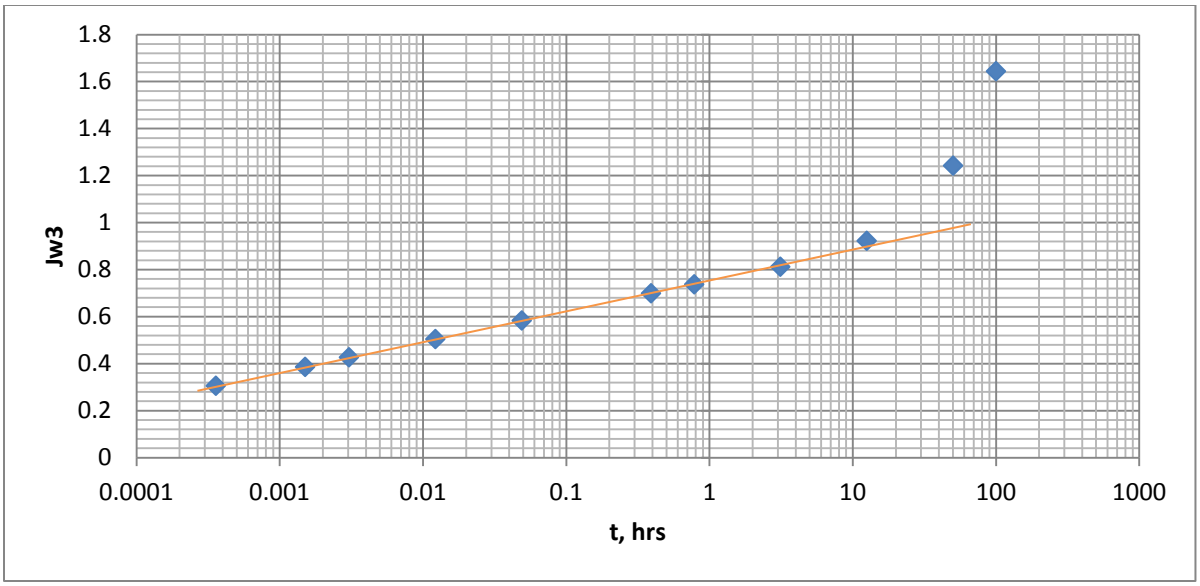

Figure 4.14: A semi-log plot of RNP against t

Figure 4.14 depicts that instead of the equivalent time function, teq, the actual time can be used for the analysis. However, if the equivalent time function, teq, is available, it is recommended to use it.

Tiab's Direct Synthesis Technique:

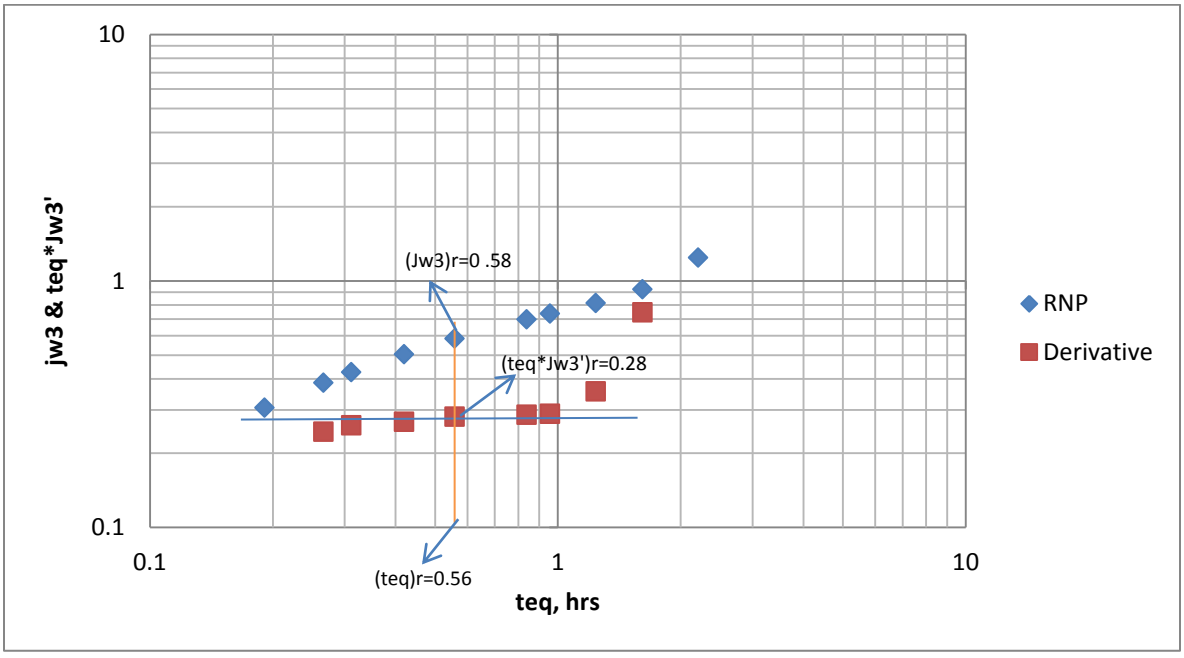

Figure 4.15: A plot of RNP and derivative against teq

From figure 4.15, $(t_{eq} * J'_{w3})_r = 0.28$

Hence the permeability of layer 3 is estimated as:

$$K_3 = \frac{70.6 * 1.0 * 1.2}{10 * 0.28} = 30.3\ mD$$

The skin layer 3 can also be estimated as:

$$s_3 = 0.5\ \frac{0.58}{0.28} - \ln\ \frac{30.3 * 0.56}{0.3 * 1 * 1.2 * 10^{-5} * 0.333\text{^}2}\ + 7.43$$

$$= -4.0$$

The solution is summarized in the following table and shows that the Tiab's Direct Synthesis has successfully been applied to the problem and is having a good match with the logarithmic convolution solution

Table 4.17: Layer 3 results for rate normalized pressure using different approaches

Parameter	Cartesian Approach	Semilog Approach	TDS
K3 (mD)	30.9	31.8	30.3
S3	-4.0	-4.0	-4.0

CHAPTER 5 DISCUSSION AND SUMMARY

5.1 Discussion

The influence of the dimensionless reservoir conductivity, $R_{CD,}$ in the pressure behavior distinguishes a multilayer reservoir from a single layer reservoir. For a single layer reservoir, R_{CD} =1, and less than 1 for multilayer reservoir. Hence, a commingled multilayered reservoir can be correlated to a single reservoir if ΔP and P'_D are plotted against t/R_{CD}^2.

For the pressure analysis, Tiab's Direct Synthesis technique was used to estimate the permeability thickness and the result was used to compare with that of the source; TDS yielded 8,825 while the source yielded 8,472. However, the actual value used in the stimulation data was 10,000. This shows that pressure data alone is not adequate in the determination of layered properties regardless of the technique used. Also, the pressure response was observed not to yield the characteristics of the individual layer properties. For example, figures 5.1 and 5.3 are similar even though they depict commingled multilayer and single layer reservoir respectively.

The analytical solution for the rate and rate derivative depicts similar characteristics as the pressure and pressure derivative analysis. This is because the surface flow rate is actually the total flow rate for the entire layers. It is useful, however, for the case of constant bottom-hole flowing pressure.

It was also shown that regardless of the flow regime (bilinear, formation linear and pseudo-radial flow), when the rate normalized pressure is differentiated with respect to the equivalent time function instead of the rate convolved time function and the derivative is plotted against the equivalent time function, a horizontal line (zero slope) is observed. This approach simplifies the analysis and precludes the need to calculate for any slope as is conventionally done. This

approach has been applied to problem 4 and was in good agreement with the other techniques. The different approaches have been found to be necessary since they give confidence in the results.

5.2 Summary

New analytic equations governing bilinear flow, linear flow and pseudo-radial flow in a finite conductivity multilayered have been developed and extended to TDS technique. Different techniques have been employed to give confidence in the result. Both fully and partially penetrating fractures have been considered in the analytic solution.

Both measured wellbore pressure and layer sandface rate are important for model identification and estimation of layered properties.

The influence function both in real-time domain and Laplace space have been derived using deconvolution. The derivation of this analytic solution precludes the assumption of a model for a particular flow regime. The deconvolved pressure and its derivative are effective tools for model identification.

An integrated approach (geological data, well testing) reduces a possible inaccurate result and helps identify both the system and model. Pressure and Pressure derivative analysis alone does not yield the layer model and leads to the estimation of the average reservoir. Individual layer properties cannot be analyzed by only pressure data.

CHAPTER 6 CONCLUSION AND RECOMMENDATION

6.1 Conclusion

1. The rate normalized pressure derivative has been found to be constant regardless of the flow regime and this precludes the need to calculate the slope. The slopes of certain flow regimes are quite close and a slight error in their computation can lead to assuming an incorrect flow regime. This method should then be of considerable value.

6.2 Recommendations

Based on the assumptions made in this research, certain recommendations could be made.

1. Initial pressure is not necessary equal in all the layers. It is essential to estimate the initial pressure of each layer for accurate estimation of layer properties.
2. Each layer may have different heterogeneity. Some layers may be naturally fractured; others may be composite while others may be homogeneous. Hence assuming homogeneities in all the layers is not always the case.
3. Crossflow fractured multilayered may also be considered.
4. Further research may also be carried out for infinite and uniform flux fractured multilayered reservoir.
5. Boundary effects should also be taken into consideration. For instance, some or all the layers may be in a closed system or intercepted be a fault (sealing or leaky). Gas cap and bottom water drive either in commingled or cross-flow will also have an effect on the pressure response and performance of multilayered reservoir.
6. Vertical well was considered in this research. Horizontal and slanted well could also be considered depending on the heterogeneities of the layers.

Nomenclature

B = Oil formation volume factor

C_{fD}= Dimensionless fracture conductivity

C_t = total compressibility

h = total reservoir thickness

h_f = fracture height

h_{fD} = Dimensionless fracture height(thickness ratio)

K = Permeability

K_o = Modified Bessel function of second kind zero order

P_D = Dimensionless pressure

P_{WD} = Dimensionless wellbore pressure

q = total flow rate

RNP or Jwj = Rate Normalized Pressure of layer j

R_{CD} = Dimensionless reservoir conductivity

RCTF or Flc = Rate Convolved Time Function of layer j

r_w = wellbore radius

r_{WD} = Dimensionless wellbore radius

S = Skin

S_{fD} = Dimensionless storage capacity of the fracture

t = time, hrs

t_D = Dimensionless time

t_{Dxf} = Dimensionless time based on fracture half length

t_{eq} = Equivalent time function

η = Hydrauliic diffusivity

u =Laplace variable

$_{WfKf}$ = Fracture conductivity

X_f = fracture half length

X_{nBL} = Rate convolved time function during bilinear flow

X_{nL} = Rate convolved time function during linear flow

Subscript

BL = Bilinear flow

D = Dimensionless

j = layer

l = linear flow

References

1. Bennett C.O., Camacho-V R.G., Reynolds A.C., Raghavan R. "Approximate Solutions for Fractured Wells Producing Layered Reservoirs", SPEJ Oct. 1985
2. Bennett C.O., Raghavan R., Reynolds A.C., "Analysis of Finite Conductivity Fractures Intercepting Multilayer Commingled Reservoirs", June 1986.
3. Camacho-V R.G., Raghavan R., Reynolds A.C., " Response of Wells Producing Layered Reservoirs: Unequal Fracture Length", SPE 12844, 1987
4. Cinco-Ley H., Samaniego F., "Transient Pressure Analysis of Fractured Wells", SPE 7490, 1981
5. Britt L.K., and Bennett C.O. "Determination of Fracture Conductivity in Moderate-Permability Reservoirs Using Bilinear Flow Concepts" SPE 14165
6. Tiab D., Bettam Y., "Practical Interpretation of Pressure Tests of Hydraulically Fractured Wells in a Naturally Fractured Reservoir", SPE 107013, 2007.
7. Lefkovits H.C., Hazabroek P., Allen E.E., Mathews C.S., " A study of the behavior of Bounded Reservoirs Composed of Stratified Layers" SPEJ March 1961.

8. Johnston J.L., Lee W.J., “Identification of Productive Layers in Low Permeability Gas Wells” JPT 21270, Nov. 1992.
9. Fernando R., Horne R.N., Cinco-Ley H., “Partially Penetrating Fractures: Pressure Transient Analysis of Infinite Conductivity Fractures” SPE 12743, 1984.
10. Igbokoyi A.O., Tiab D., “Pressure Transient Analysis in Partially Penetrating Infinite Conductivity Hydraulic Fractures in Natural Fractured Reservoirs”, SPE 116733, 2008.
11. Tiab D., Bettam Y., “Practical Interpretation of Pressure Tests of Hydraulically Fractured Wells in a Naturally Fractured Reservoir”, SPE 107013, 2007.
12. Gringarten A.C., Ramey H.J., “The Use of Source and Green’s Functions in Solving Unsteady-Flow Problems in Reservoirs”, SPE 3818, Oct 1973.
13. Rodriguez F., R.N. Horne, and Cinco-Ley, “Partially Penetrating Vertical Fractures: Pressure Transient Behavior of a finite-Conductivity Fracture”
14. Raghavan R., Uraiet, A. and Thomas G.W., “Vertical Fractured Height: Effect on Transient Flow Behavior”, SPE 6016, Aug. 1978.
15. Christine A. Ehlig-Economides and Jeffrey Joseph, “A New Test of Determination of Individual Layer Properties in a Multilayered Reservoir”, SPE 14167, Sept. 1987.
16. C. Ehlig-Economides and J. Joseph, “Evaluation of Single-Layer Transients in a Multilayered System”, SPE 15860, Oct., 1986.
17. Kuchuk, F.J., Carter R.G., Ayesteran L., “Deconvolution of Wellbore Pressure and Flow Rate”, SPE 13960, March, 1990.
18. Christine A. Ehlig-Economides, “Testing and Interpretation in Layered Reservoirs”, 1987.

19. C.U. Okoye, A.D. Oshinnuga and A. Ghalambor, “Pressure Transient Behavior of Vertically Fractured Wells in a Closed Square Multilayered Reservoir”, March 1990.
20. Gao, C., Jones, J.R., Raghavan, R., John Lee W., “Responses of Commingled Systems With Mixed Inner and Outer Boundary Conditions Using Derivatives”, SPE 22681, Dec., 1994.
21. Gao, C., Jones, J.R., Raghavan, R., John Lee W., “ Supplement to SPE 22681.Interpretation of Responses of Commingled Systems With Mixed Inner and Outer Boundary Conditions Using Derivatives”, SPE 30070, 1994.
22. Christine A. Ehlig-Economides, “Model Diagnosis for Layered Reservoirs”, SPE 20923, Sept., 1993.
23. Peres A.M.M., Reynolds A.C., “A new General Pressure-Analysis Procedure for Slug Test”, December, 1993.
24. Osman, M.E., “Well Testing of a Fractured Well in a Multilayered Bounded Square”, SSPE 24961, 1992.
25. Kuchuk, F., Karakas, M., Ayestaran, L.,“Well Testing and Analysis Techniques for Layered Reservoirs”, SPE 13081, August, 1986
26. Otuomagie, R., Menzie D.E., “Analysis of Pressure Buildup in an Infinite Two-Layered Oil Reservoir without Crossflow”, SPE 6130, Oct., 1976.
27. Bourdet D., “Pressure Behavior of Layered Reservoirs with Crossflow”, SPE 13628, March, 1985.
28. Rushing, J.A., Blasingame, T.A., Johnston J.L., John Lee, W., “Slug Testing in Multiple Coal Seams Intersected by a Single, Vertical Fracture”, SPE 22945, Oct., 1991.

29. Gao, C., “Determination of Individual Layer Properties by Layer-by-layer Well Tests in Multilayered Reservoirs with Crossflows”, SPE 15321, 1985.
30. J.B. Spath, E. Ozkan, R. Raghavan “An Efficient Algorithm for Computation of Well Responses in Commingled Reservoirs”, SPE 21550, June 1990.
31. J.B. Spath, E. Ozkan, R. Raghavan, “Supplement to SPE 21550. An Efficient Algorithm for Computation of Well Responses in Commingled Reservoirs”, SPE 29156. 1994.
32. M.E. Osman, “Transient Pressure Analysis for Wells in Multilayered Reservoir with Finite Conductivity Fractures”, SPE 25665, April 1993.
33. A. Mongi, D. Tiab, “Application of Tiab’s Direct Synthesis Technique to Multi-Rate Tests”, SPE 62607, June 2000.
34. F., Kuchuk and L. Ayestaran, “Analysis of Simultaneously Measured Pressure and Sandface Flow Rate in Transient Well Testing”, February, 1985.
35. G. Chang-Tai, “Determination of Parameters of Individual Layers in Multilayer Reservoirs by Transient Well Tests”, Paper No. 86-37-82, Petroleum Society of CIM, June 1986.
36. P.C. Shah and J.B. Spath, “Transient Wellbore Pressure and Flow Rates in a Commingled System with Different Layer Pressures”, SPE 25423, March, 1993.
37. P.C. Shah, M. Karakas, F. Kuchuk, L.C. Ayesteran, “Estimation of the Permeabilities and Skin Factors in Layered Reservoirs with Downhole Rate and Pressure Data”, SPE 14131, Sept., 1988.
38. M. Eissa, S. Joshi, K. Singh, A. Bahuguna, M. Elbadri, “Identifying Layer permeabilities and Skin Using a Multi-Layer Transient Testing Approach in a Complex Reservoir Environment”, SPE 116969, November, 2008.

39. F.J. Kuchuk, P.C. Shah, L. Ayestaran, B. Nicholson, “Application of Multilayer Testing and Analysis: Afield Case”, SPE 15419, October 1986.
40. I.S. Nashawi, A. Mallalah, “Rate Derivative Analysis of Oil Wells Intercepted by Finite Conductivity Hydraulic Fracture”,
41. A. Mallalah, I.S. Nashawi, M. Algharaib “Constant-Pressure Analysis of Oil Wells Intercepted by Infinite-Conductivity Hydraulic Fracture Using Rate and Rate-Derivative Functions” SPE 105046, March 2007.
42. A.F. van Everdingen, W. Hurst, “The Application of the Laplace Transformation to Flow Problems in Reservoirs”, SPE 949305, December, 1949.
43. C.W. Morris “Case Study of a Gulf Coast Layered Reservoir Using Multirate Transient Testing”, SPE 16762, 1987.
44. L. Larsen, “Determination of Skin factors and Flow Capacities of Individual Layers in Two-Layered Reservoirs”, SPE 11138, Sept., 1982.
45. L. Larsen, “Experiences with Combined Analysis of PLT and Pressure-Transient Data from Layered Reservoirs”, SPE 27973, August 1994.
46. M.J.Mavor, G.W. Walkup Jr., “Application of Parallel Resistance Concept to Well Test Analysis in Multilayered Reservoirs”, SPE 15117, April 1986.
47. Cheng-Tai Gao, H.A.Deans, “Pressure Transients and Crossflow Caused by Diffusivities in Multilayered Reservoirs”, SPE 11966, June 1988.
48. F.J. Kuchuk, D.J.Wilkinson, “Transient Pressure Behavior of Commingled Reservoirs”, SPE 18125, March 1991.
49. C.U. Okoye, A.D. Oshunga, Ghalambor, U., “Pressure Transient Behavior in Multilayer Vertically Fractured Gas Reservoir with Finite Conductivity” SPE 18960, March 1989.

50. J.L. Johnston, W.J. Lee, “Identification of Productive Layers in Low Permeability Gas-Wells”, SPE 21270, Nov., 1992.
51. T.C. Ryan, M.J. Sweeney, W.H. Jamieson Jr., J.J. Tanigawa, “Individual Layer Transient Tests in Low Pressure, Multi-Layered Reservoirs”, SPE 27928, May 1994.
52. C.L. Jordan, L. Mattar, “Comparison of Pressure Transient Behavior of Composite and Multi-Layer Reservoir”, CIPC 2000-45, June 2000.
53. J. Joseph, A. Bocock, F. Nai-Fu, L.T. Gui, “A Study of Pressure Transient Behavior in Bounded Two-Layered Reservoirs: Shengli Field China”, SPE 15418, Oct., 1986.
54. W.M. Cobb, H.J. Ramey Jr., F.G. Miller, “Well Test Analysis for Wells Producing Commingled Zones”, SPE 3014, January, 1972.
55. R.E. Gladfelter, G.W. Tracey, L.E. Wilsey, “Selecting Wells which will Respond to Production-Stimulation Treatment” March 1955.
56. Yan Pan, M. Sullivan, D. Belanger, “Best Practices in Testing and Analyzing Multilayer Reservoir”, SPE 132596, May, 2010.
57. R.B.Sullivan, W.J.Lee, S.A. Holditch, “Pressure Transient Response in Multilayer Gas Reservoirs Containing Hydraulic Fractures”, SPE 16399, May 1987.
58. Prijambodo R., Raghavan., Reynolds, A., “Well Test Analysis for Wells Producing Layered Reservoirs with Crossflow”, SPE, June 1985

Appendix A

Derivation of the analytical solution during pseudo-radial flow in commingled reservoirs

The radial diffusivity equation in terms of layer properties is given by

$$\frac{1}{r_D}\frac{\partial}{\partial r_D}\left[r_D\frac{\partial P_{Dj}}{\partial r_D}\right]=\frac{1}{\eta_{Dj}}\frac{\partial P_{Dj}}{\partial t_{Dxf}} \qquad (A-1)$$

Taking Laplace transforms of both sides of equation (3.2.50)

$$\frac{\partial^2 P_{Dj}}{\partial r_D^2}+\frac{1}{r_D}\frac{\partial P_{Dj}}{\partial r_D}=\frac{1}{\eta_{DJ}}\left[uP_{Dj}-P_{Dj}\left[t_D=0\right]\right]=0 \qquad (A-2)$$

Initial condition for layer j;

$$P_{Dj}\left[t_D=0\right]=0 \qquad (A-3)$$

Hence equation (3.2.52) becomes

$$\frac{\partial^2 P_{Dj}}{\partial r_D^2}+\frac{1}{r_D}\frac{\partial P_{Dj}}{\partial r_D}=\frac{1}{\eta_{DJ}}\left[uP_{Dj}\right] \qquad (A-4)$$

Now, let $u_j=\left[1\ \eta_{DJ}\right]u$ $\qquad (A-5)$

$$\frac{\partial^2 P_{Dj}}{\partial r_D^2}+\frac{1}{r_D}\frac{\partial P_{Dj}}{\partial r_D}=u_jP_{Dj} \qquad (A-6)$$

The solution to equation (A-6) assuming a line source well in an infinite acting commingled reservoir is as given in equation in the main text.